MICROCOPY RESOLUTION TEST CHART
NATIONAL BUREAU OF STANDARDS-1963-

NAVAL POSTGRADUATE SCHOOL
Monterey, California

DTIC
S ELECTE D
MAR 1 1 1988
C&D

THESIS

THE PHYSICAL OCEANOGRAPHY
OF THE
NORTHERN BAFFIN BAY-NARES STRAIT REGION

by

Victor G. Addison, Jr.

December 1987

Thesis Advisor   R.H. Bourke

Approved for public release; distribution is unlimited.

88 3 10 022

NAVAL POSTGRADUATE SCHOOL
Monterey, California

Rear Admiral R. C. Austin   Kneale T. Marshall
Superintendent   Acting Provost

   This thesis was prepared in conjunction with research sponsored by the
Arctic Submarine Laboratory, Naval Ocean Systems Center, San Diego, California
under Work Order N66001-86-WR-00131. Reproduction of all or part of this
report is authorized.

                              Released by:

                              Gordon E. Schacher
                              Dean of Science and Engineering

REPORT DOCUMENTATION PAGE

REPORT SECURITY CLASSIFICATION UNCLASSIFIED	1b RESTRICTIVE MARKINGS		
SECURITY CLASSIFICATION AUTHORITY	3 DISTRIBUTION/AVAILABILITY OF REPORT Approved for public release;		
DECLASSIFICATION/DOWNGRADING SCHEDULE	distribution is unlimited.		

PERFORMING ORGANIZATION REPORT NUMBER(S) NPS 68-87-008	5 MONITORING ORGANIZATION REPORT NUMBER(S)		

NAME OF PERFORMING ORGANIZATION Naval Postgraduate School	6b OFFICE SYMBOL *(If applicable)* Code 68	7a NAME OF MONITORING ORGANIZATION Arctic Submarine Laboratory		
ADDRESS (City, State, and ZIP Code) Monterey, CA 93943-5000		7b ADDRESS (City, State, and ZIP Code) Code 19, Bldg. 371 Naval Ocean Systems Center San Diego, CA 92152		

NAME OF FUNDING/SPONSORING ORGANIZATION Arctic Submarine Laboratory	8b OFFICE SYMBOL *(If applicable)* Code 19	9 PROCUREMENT INSTRUMENT IDENTIFICATION NUMBER N6600186WR00131		

ADDRESS (City, State and ZIP Code) Bldg. 371 Naval Ocean Systems Center San Diego, CA 92152	10 SOURCE OF FUNDING NUMBERS			
	PROGRAM ELEMENT NO	PROJECT NO	TASK NO	WORK UNIT ACCESSION NO

TITLE (Include Security Classification)

THE PHYSICAL OCEANOGRAPHY OF THE NORTHERN BAFFIN BAY-NARES STRAIT REGION

PERSONAL AUTHOR(S)
Addision, Victor G., Jr.

13a TYPE OF REPORT Master's Thesis	13b TIME COVERED FROM_____ TO_____	14 DATE OF REPORT (Year, Month, Day) 1987 December	15 PAGE COUNT 110

SUPPLEMENTARY NOTATION

Prepared in conjunction with R.H. Bourke and R.G. Paquette

COSATI CODES			18 SUBJECT TERMS (Continue on reverse if necessary and identify by block number)	
FIELD	GROUP	SUB-GROUP	Baffin Bay Nares Strait	SIR JOHN FRANKLIN North Water

ABSTRACT (Continue on reverse if necessary and identify by block number)

A dense network of conductivity-temperature-depth (CTD) measurements was conducted from Baffin Bay northward to $82°09'N$ at the entrance to the Lincoln Sea, in most comprehensive physical oceanographic survey ever performed in the northern Baffin Bay-Nares Strait (NBB-NS) region. These data indicate Nares Strait Atlantic Intermediate Water (NSAIW) and Arctic Basin Polar Water (ABPW) to be derived from Arctic Basin waters via the Canadian Archipelago, whereas the West Greenland (WGC) is the source of the comparatively dilute West Greenland Current Atlantic Intermediate Water (WGCAIW) and West Greenland Current Polar Water (WGCPW) fractions. Baffin Bay Surface Water (BBSW) is found seasonally throughout northern Baffin Bay. Recurvature of component branches of the WGC, which attains a maximum baroclinic transport of 0.7 Sv, occurs primarily in Melville Bay (0.2 Sv), south of the Carey Islands (0.1 Sv) and ultimately in Smith Sound (0.2 Sv). The Baffin Current originates as an ice-edge jet in Smith Sound and is augmented by net outflow from Smith, Jones, and Lancaster Sounds at rates of 0.3 Sv, 0.3 Sv and 1.1 Sv, respectively. Circulation in Smith, Jones and

DISTRIBUTION/AVAILABILITY OF ABSTRACT ☒ UNCLASSIFIED/UNLIMITED ☐ SAME AS RPT ☐ DTIC USERS	21 ABSTRACT SECURITY CLASSIFICATION UNCLASSIFIED	
NAME OF RESPONSIBLE INDIVIDUAL R.H. Bourke	22b TELEPHONE (Include Area Code) (408) 646-3270	22c OFFICE SYMBOL 68Bf

Block 18 (continued)

Geostrophic Estuarine Circulation   Smith Sound
Lancaster Sound   Kane Basin
Jones Sound   Melville Bay

Block 19 (continued)

Lancaster Sounds can be described in terms of the Geostrophic Estuarine
Circulation Model (GEC). The North Water is caused by the combined influences
of near-surface layer enthalpy and mechanical ice removal.

Accesion For

NTIS CRA&I	✔
DTIC TAB	☐
Unannounced	☐
Justification	

By
Distribution/

Availability Codes

| Dist | Avail and/or Special |
| A-1 | |

The Physical Oceanography of the
Northern Baffin Bay-Nares Strait Region

by

Victor G. Addison, Jr
Lieutenant, United States Navy
B.S., State University of New York, Stony Brook, 1979

Submitted in partial fulfillment of the
requirements for the degree of

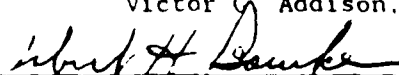MASTER OF SCIENCE IN METEOROLOGY AND OCEANOGRAPHY

from the

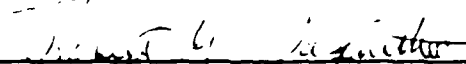NAVAL POSTGRADUATE SCHOOL
December 1987
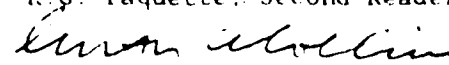
Author: _____

Victor G. Addison, Jr.

Approved by: _____

R.H. Bourke, Thesis Advisor

_____

R.G. Paquette, Second Reader

_____

C.A. Collins, Chairman
Department of Oceanography

_____

Gordon E. Schacher
Dean of Science and Engineering

3

ABSTRACT

A dense network of conductivity-temperature-depth (CTD) measurements was conducted from Baffin Bay northward to $82°09'N$ at the entrance to the Lincoln Sea, in the most comprehensive physical oceanographic survey ever performed in the northern Baffin Bay-Nares Strait (NBB-NS) region. These data indicate Nares Strait Atlantic Intermediate Water (NSAIW) and Arctic Basin Polar Water (ABPW) to be derived from Arctic Basin waters via the Canadian Archipelago, whereas the West Greenland Current (WGC) is the source of the comparatively dilute West Greenland Current Atlantic Intermediate Water (WGCAIW) and West Greenland Current Polar Water (WGCPW) fractions. Baffin Bay Surface Water (BBSW) is found seasonally throughout northern Baffin Bay. Recurvature of component branches of the WGC, which attains a maximum baroclinic transport of 0.7 Sv, occurs primarily in Melville Bay (0.2 Sv), south of the Carey Islands (0.1 Sv) and ultimately in Smith Sound (0.2 Sv). The Baffin Current originates as an ice-edge jet in Smith Sound and is augmented by net outflow from Smith, Jones, and Lancaster Sounds at rates of 0.3 Sv, 0.3 Sv and 1.1 Sv, respectively. Circulation in Smith, Jones and Lancaster Sounds can be described in terms of the Geostrophic Estuarine Circulation Model (GEC). The North Water is caused by the combined influences of near-surface layer enthalpy and mechanical ice removal.

4

TABLE OF CONTENTS

5

LIST OF TABLES

7

LIST OF FIGURES

9

ACKNOWLEDGEMENTS

11

I. INTRODUCTION

A. PURPOSE

During September 1986, the CCGS SIR JOHN FRANKLIN conducted an oceanographic measurement program from Baffin : ay northward into Nares Strait, to the southern reaches of the Lincoln Sea. This expedition marked the first comprehensive use of continuous profiling conductivity-temperature-depth (CTD) measurements throughout the region, and the northernmost transit (82°09′N) of a surface ship through Nares Strait since the 1971 voyage of the CCGS LOUIS S. ST. LAURENT. Sponsorship of this endeavor was provided by the Arctic Submarine Laboratory, with diplomatic concurrence from the governments of Canada and Denmark.

The principal objective of the cruise was to examine the distribution of physical oceanographic variables from Baffin Bay northward, in order to determine the circulation and water mass characteristics of the region. The successful transit of the region by the SIR JOHN FRANKLIN provides a data set from which it is possible, essentially for the first time, to thoroughly define the baroclinic circulation and water mass structure of the northern Baffin Bay-Nares Strait region.

Specific objectives of the analysis will be to: (1) define the trajectory, transport and extent of the West Greenland and Baffin Currents; (2) describe the characteristics and extent of the water masses found throughout the region; (3) characterize the role of topographic steering and bathymetric boundaries on baroclinic

12

circulation and water mass penetration; (4) present a model which
explains the observed circulation in Smith, Jones, and Lancaster
Sounds; and (5) present a hypothesis for the formation and maintenance
of the North Water, a large polynya located in Northern Baffin Bay.

B.   BACKGROUND

The northern Baffin Bay-Nares Strait (hereinafter referred to as
NBB-NS) region is historically significant for a number of seemingly
unrelated reasons (Figure 1.1). Lancaster Sound, noted as the
traditional Atlantic entrance to the Northwest Passage and as a net
source of Arctic Ocean water inflow to the region, remains relatively
ice free during winter. Indeed, northern Baffin Bay as a whole was
thought to remain conspicuously unencumbered by ice during the winter
due to the presence of the North Water. The Humboldt Glacier, the
largest glacier in the northern hemisphere, is located on the eastern
side of Nares Strait and is the source for many of the icebergs which
are observed throughout the NBB-NS region. Once calved from the
glacier, many of these icebergs travel southward past Cape York, in
defiance of the northward flowing West Greenland Current. The most
comprehensive oceanographic analysis of the northern Baffin Bay region
is provided by Muench (1971). Muench's work serves as a summary of all
significant oceanographic research conducted prior to 1971, and has been
referenced in all subsequent analyses of the NBB-NS region.

Prior to 1972, all baroclinic oceanographic analyses in the NBB-NS
region were derived from bottle sampling techniques. The CCGS LOUIS S.
ST. LAURENT obtained discrete measurements of temperature and salinity
in Nares Strait during August 1971, reaching a latitude of 82°56'N

13
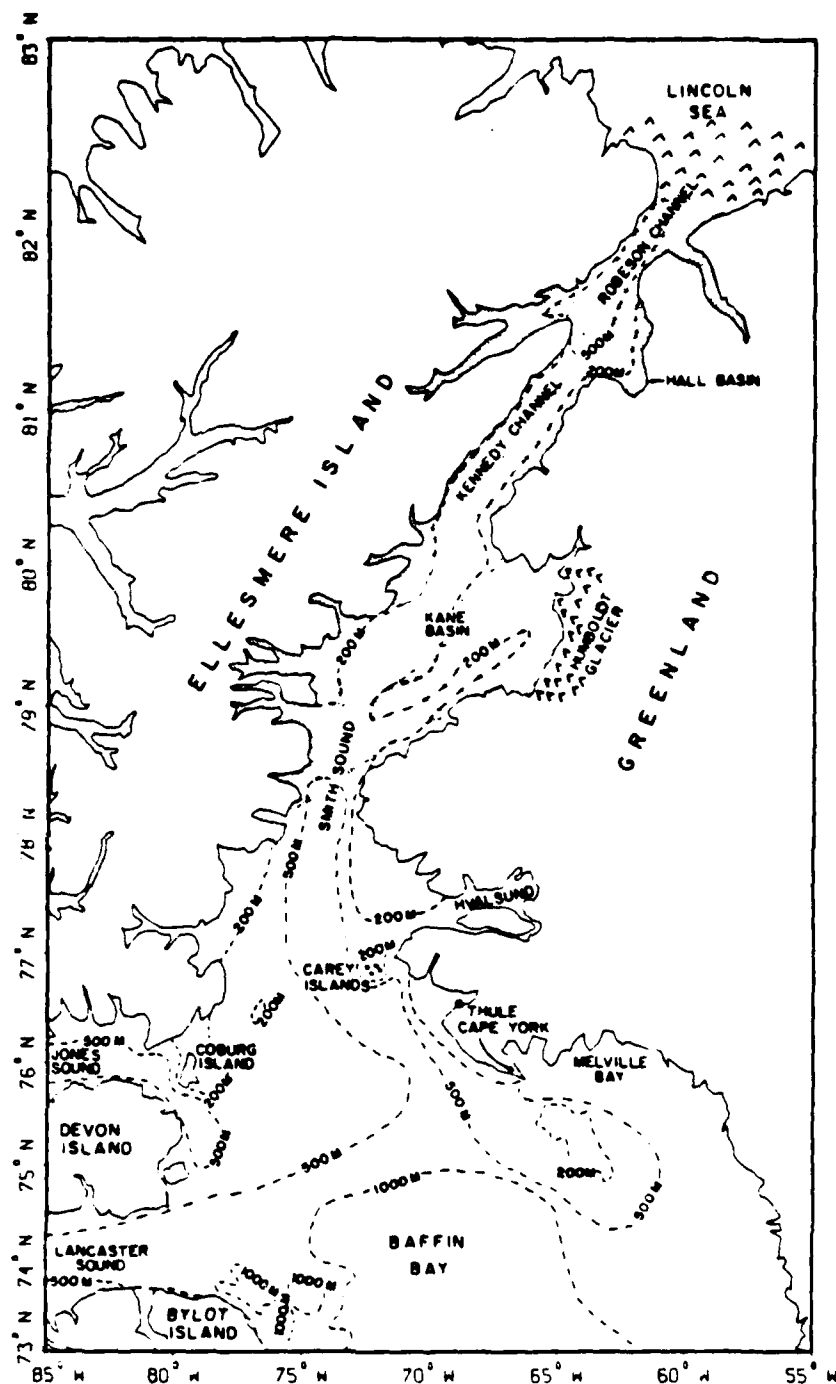
Figure 1.1   A chart of the northern Baffin Bay-Nares
              Strait region. Ice concentrations greater than
              7/10 (during the FRANKLIN 86 cruise) are
              represented as shaded areas.

14

(Sadler, 1976). During 1972, scientific personnel aboard the LOUIS S. ST. LAURENT obtained the first winter oceanographic data from Davis Strait utilizing an in situ salinity/temperature/depth unit (STD) (Muench and Sadler, 1973). Transports through Nares Strait have been investigated by Sadler (1976), providing the most accurate current meter derived estimates of Lincoln Sea inflow to the region. In 1978 and 1979, the Eastern Arctic Marine Environment Studies (EAMES) program utilized current meters and CTD stations to investigate the southward flowing Baffin Current (Fissel et al., 1982). Research concerning the processes leading to the formation of the North Water has most recently been conducted by Steffen and Ohmura (1985).

1. **Bathymetry**

The bottom topography of the NBB-NS region is complex and, as such, has the potential to exert significant control over physical oceanographic processes. The influence of glaciers on all aspects of the morphology of this region is quite obvious.

Northern Baffin Bay is fed by Lancaster and Jones Sounds to the west, and Smith Sound to the north. Shoaling to depths of less than 200 m occurs at some point in both Lancaster and Jones Sounds, effectively restricting deeper Arctic Ocean inflow. A sill which ranges in depth from 160 m to 200 m is present at the southern end of Kennedy Channel, providing similar constraints on Lincoln Sea inflow to the region. Similarly, shoaling to a depth of 250 m occurs at the Smith Sound entrance to Kane Basin.

The deep, relatively flat central portion of northern Baffin Bay is punctuated in its eastern portion by a shallow (700 m) bank

15

located in Melville Bay. A deep (500 m to 900 m) channel passes offshore from Cape York, terminating northward in Smith Sound. To the west, the mouths of Jones and Lancaster Sounds reach depths of 700 m, but the bottom northeast of Devon Island shoals to less than 200 m approaching Smith Sound.

2. General Circulation

The baroclinic circulation pattern in the NBB-NS region is dominated by the northward flowing West Greenland Current (WGC) and the southward flowing Baffin Current (Figure 1.2). Augmenting the transport of the Baffin Current are net outflows from Jones and Lancaster Sounds, coupled with southward flow through Nares Strait. The net baroclinic transport through northern Baffin Bay has been computed to be approximately 2.0 Sv ($10^6 m^3 s^{-1}$) southward (Muench, 1971). Muench postulated that this transport is driven by a higher surface elevation in the Arctic Ocean relative to that in Baffin Bay, presumed to be a consequence of differing water structures in their respective upper 250 m layers.

Bottom topography, predominantly northerly winds, and meltwater admixture are thought to play variable roles in the maintenance of a cyclonic circulation pattern in northern Baffin Bay. The WGC, a significantly barotropic current, may be enhanced baroclinically by near-shore low salinity wedges of meltwater. Alternately, the Baffin Current exhibits the increased baroclinic intensity characteristically found in western boundary currents. The westward turning of the WGC off Cape York, and the southward turning of Lancaster Sound outflow are both influenced by topographic steering (Church, 1 1)

16
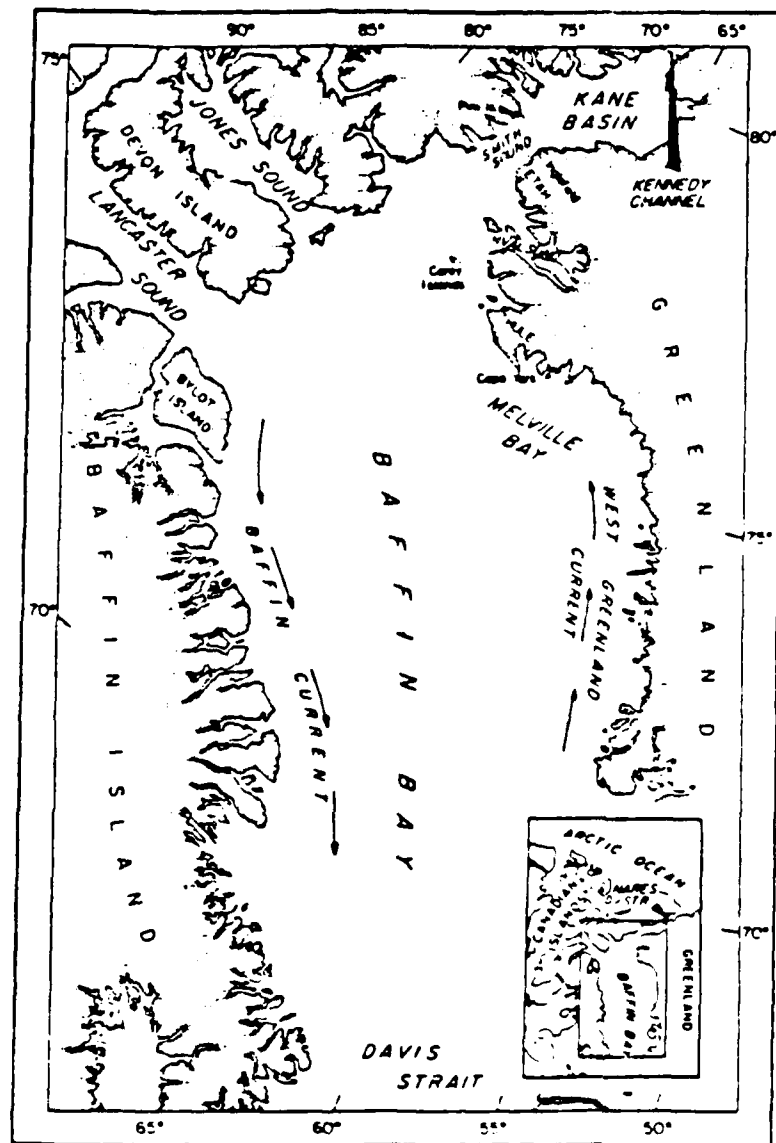
Figure 1.2   The West Greenland Current and the Baffin
                      Current (from Muench, 1971, p. 2).

Circulation features in the NBB-NS region may be subject to seasonal variations. Lemon and Fissel (1982) noted a general winter weakening of near-surface baroclinic currents by a factor of two or more. The WGC, which transports northward only 10% of the baroclinic volume transported southward by the Baffin Current, is not always present during late summer (Muench, 1971).

The directional components of some features of the surface and baroclinic flow fields are temporally variable. Muench stated that reversals of baroclinic flow have been observed in Smith and Jones Sounds, while reversals of surface flow have occurred in Smith Sound. Lancaster Sound, however, consistently provides net inflow to Baffin Bay on the order of twice that of Smith or Jones Sounds (Muench, 1971). Anticyclonic eddies (sometimes referred to as counter currents) have been reported near Bylot Island (Fissel et al., 1982), while cyclonic eddies have been observed off Cape York (Muench, 1971).

Current speeds in the NBB-NS region, although variable, are consistently greatest in magnitude near eastern Lancaster Sound. Fissel et al. (1982), using current meters, found near-surface velocities of 0.75 m/sec in the portion of the Baffin Current located east of Lancaster Sound. Directly measured current speeds in Nares Strait are extremely variable in magnitude, with maximum near-surface values ranging from 0 1 to 0.60 m/sec (Sadler, 1976). Maximum baroclinic velocities in the WGC are on the order of 0 1 m/sec (Muench, 1971).

The nature and vertical extent of the flow regimes in the NBB-NS region are spatially complex. Although the vertical extent of volume flow in the WGC probably reaches a depth of 200 m most

baroclinic flow is limited to the upper 100 m (Muench, 1971). The
Baffin Current nominally extends to a depth of 500 m, with flow reaching
the bottom (700 m to 840 m deep) in the region of its intrusion into
Lancaster Sound (Fissel et al., 1982). Significant baroclinic flow in
this current is associated with the upper few hundred meters (Muench,
1971). The flow in Nares Strait has a substantial baroclinic component
which reaches to depths of 300 m (Sadler, 1976).

3. Water Masses

Adopting the usual convention for Arctic regions, Muench (1971)
divided the waters of northern Baffin Bay into three layers: a cold
($<0°$C) upper Arctic Water layer; a warmer ($>0°$C) intermediate-depth
Atlantic Water layer; and a cold ($<0°$C) Deep Water Layer. The Arctic
Water, confined to the upper 200 m to 300 m, has an upper limit in
salinity of approximately 34.0. The Atlantic Water extends from the
bottom of the Arctic Water layer to depths of 700 m in Lancaster Sound
and 1300 m in northern Baffin Bay, exhibiting salinities of 34.2 to
34.5. Baffin Bay Deep Water extends from the bottom of the Atlantic
Layer to the seabed, and is characteristically isohaline at 34.48.

The density of water masses in the NBB-NS region, as in other
Arctic regions, is primarily determined by salinity. Surface and near-
surface layers, therefore, are usually characterized by strong
haloclines and associated pycnoclines. The delineation of a surface
(upper 75 m) layer of Arctic Water, which is modified by boundary layer
processes, has been suggested by Fissel et al. (1982). Since diverse
processes such as solar heating, meltwater admixture, and wind mixing

play roles in the formation of this layer, its temperature and salinity characteristics vary seasonally.

The thermohaline characteristics of the water masses of the region can generally be traced to their sources, while their horizontal extent is often determined by bathymetric effects. Arctic Water is water of Arctic Ocean origin which either entered Baffin Bay via Davis Strait and was modified by cooling and admixture of runoff within northern Baffin Bay, or was modified by cooling and freshening within the Arctic Ocean prior to entering Baffin Bay from the north. Mixing of inflowing Arctic Ocean Water and resident Baffin Bay Arctic Water of the same density occurs in southern Smith Sound, Jones Sound, and Lancaster Sound. Shallow sills present in Lancaster Sound, Jones Sound and Kennedy Channel prevent southward flow of Arctic Ocean Atlantic Water into Baffin Bay. Atlantic Water in northern Baffin Bay, therefore, originates from the Atlantic Ocean via Davis Strait (Muench, 1971).

4. The North Water

Extensive interest has been focused on a persistent polynya, termed the North Water, which is located in northern Baffin Bay (Figure 1.3). Dunbar (1970) concluded that the polynya is defined by a stable northern boundary at the Smith Sound entrance to Kane Basin, and a consistent western ice edge which forms along Ellesmere Island. The locations of the eastern and southern boundaries are seasonally dependent. Significant penetration of the North Water occurs westward into Lancaster Sound in June. The phenomenon is less well defined during the summer season after ice break up commences. Contrary to earlier reports, the North Water is never completely open during
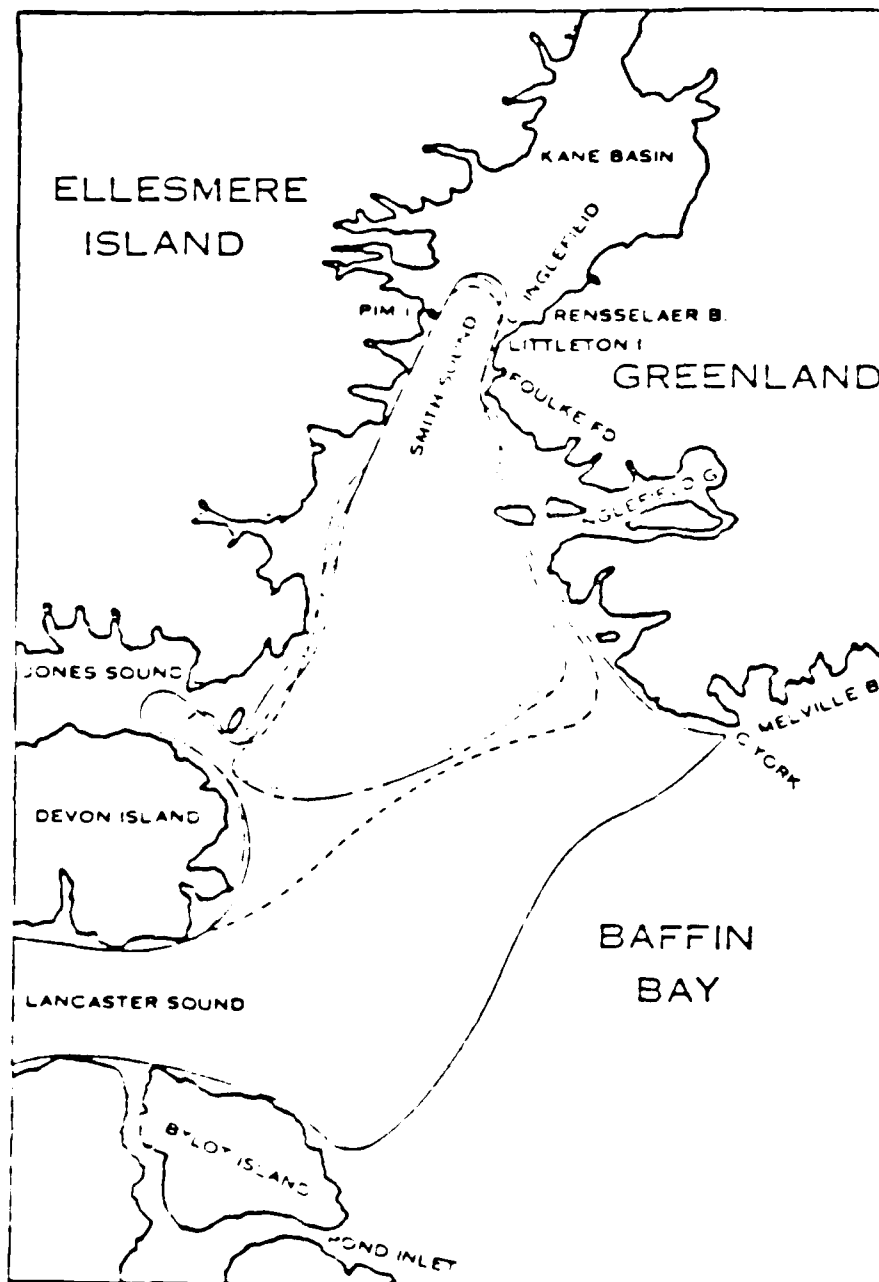
Figure 1.3   The approximate mean monthly extent of the North
                    Water in: March (.....), April (_ _ _ _), May
                    (- - -), June (____); (from Dunbar, 1970, p.
                    279).

21

winter, and is characterized by extensive areas of new ice formation (Dunbar, 1973). Steffen and Ohmura (1985) used thermal infrared measurements from an airplane in winter to determine that the North Water was mostly covered with new and young ice, and probably devoid of first year ice until March. The ice surface, they surmised, was approximately 20°C warmer than that of the surrounding fast ice.

The North Water essentially remains an unexplained phenomenon. Muench (1971) computed a heat budget for the region and concluded that insufficient heat is present in the Atlantic Water layer in northern Baffin Bay to prevent ice formation. He similarly concluded that there was not enough heat present in the surface Arctic Water layer either, and postulated mechanical ice removal by northerly winds and currents as the effects responsible for the formation of the North Water. Dunbar (1973) reinforced this hypothesis by noting that the age and thickness of ice increases from the Smith Sound ice arch southward. Steffen and Ohmura (1985), however, computed more accurate heat budgets for the region and concluded that oceanic heat of unknown origin is responsible for the formation and maintenance of this polynya.

II. METHODS AND MEASUREMENTS

A. CRUISE SUMMARY

Between 7 and 27 September 1986, the CCGS SIR JOHN FRANKLIN
conducted the most extensive physical oceanographic survey ever
performed in the NBB-NS region. The SIR JOHN FRANKLIN covered over
4000 km in the course of conducting 145 CTD stations (Figure 2.1; refer
to Figure 2.2 for station number identification). Numerous transects
were performed while transiting from Lancaster Sound northward to
Robeson Channel, and subsequently southward to Melville Bay. Ice
reconnaissance was provided by the SIR JOHN FRANKLIN's embarked
helicopter, which was instrumental in enabling the ship to penetrate
Robeson Channel to 82°09'N; the furthest northward of any ice breaker
since 1972.

B. INSTRUMENTATION

The instruments used were the Applied Micro Systems Limited
Conductivity-Temperature-Depth recorder, model STD-12. This instrument
has a stated accuracy of 0.02 mS/cm in electrical conductivity, 0.01°C
in temperature and no stated accuracy in depth. The resolutions were
stated to be 0.003 mS/cm, 0.001°C, and 0.05 dbar, respectively.

Three instruments, numbered 422, 433 and 467, respectively, were
utilized during the cruise. CTD #433 is the property of the Naval
Postgraduate School (NPS), and was calibrated both before and after the
cruise with resultant errors of 0.003°C in temperature and 0.007 mS/cm
in conductivity. Calibrations for the other two instruments were not
initially available, and were obtained empirically in the form of first

23
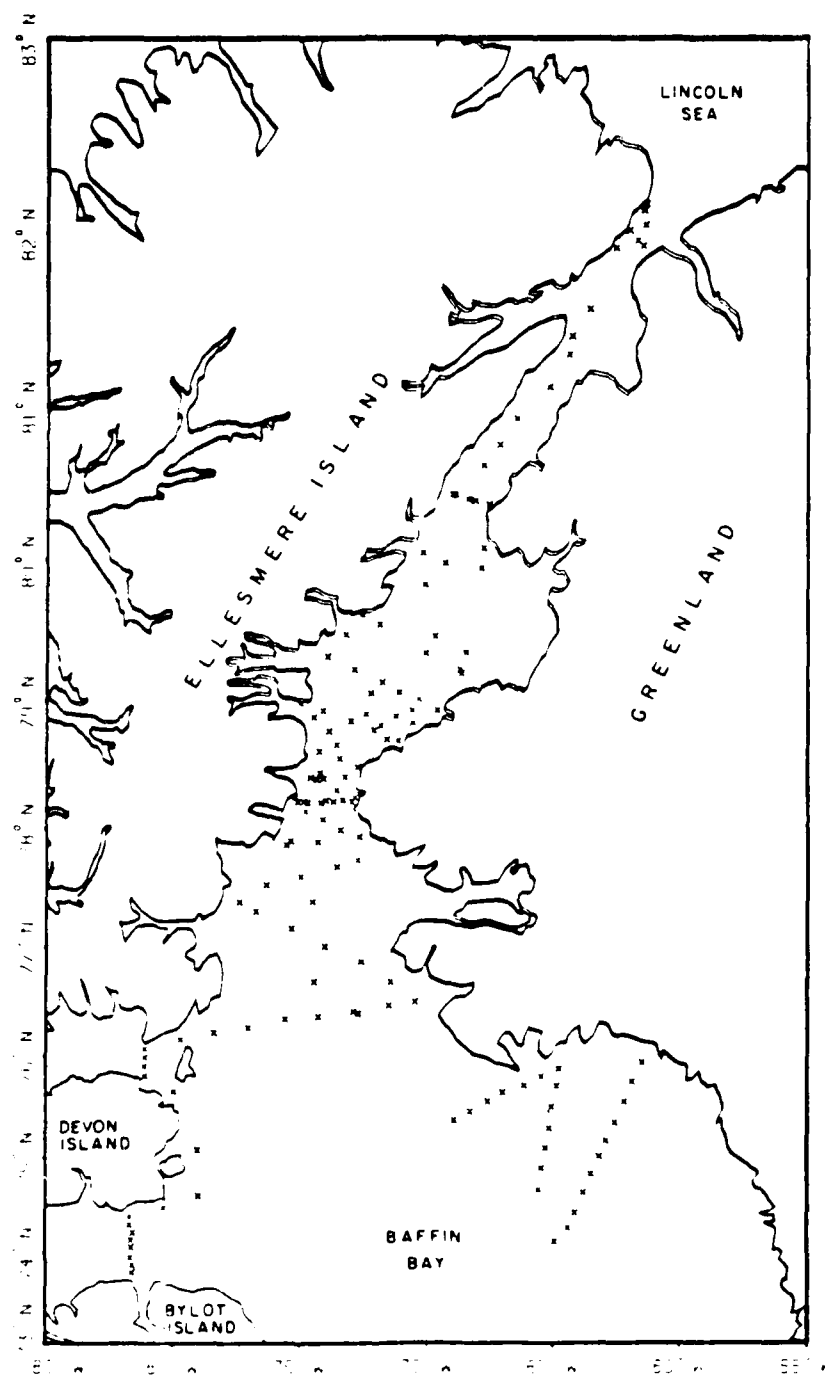
Figure 2.1   The locations of CTD stations conducted during the
September 1986 cruise of CCGS SIR JOHN FRANKLIN.

24

degree polynomials by intercomparison with CTD #433 during simultaneous lowerings. It is concluded that the absolute error in the variables issmaller than $0.02°C$, 0.02 mS/cm, and 2.0 dbars. The root mean square error in salinity, therefore, is approximately 0.03.

The data were recorded internally in coded binary form, and were downloaded into a Compaq computer for conversion into engineering units and storage on 5.25 in. floppy diskettes. Each CTD was programmed to sample the data stream every 0.8 dbar of pressure change. Significantly finer resolution in pressure was not convenient because of computer memory limitations and downloading time constraints.

The primary navigation aid was the ship's Magnavox MX 1107 Satellite Navigation System. An average of two fixes per hour provided a mean navigational accuracy of 0.5 km.

C. DATA REDUCTION AND ANALYSIS

Upon completion of the cruise, the data were transferred to mass storage cartridges for further processing with the NPS IBM 3033 computer. Editing of spurious and mis-sequenced data points, the cause of which is discussed by Tunnicliffe (1985), was subsequently performed. Removal of dynamic response errors in temperature and salinity was accomplished as prescribed by Bourke et al. (1986). The edited profile data were then sub-sampled every 5 m for use in the production of baroclinic velocity profiles and related volume transport estimates.

Transects used in the data analysis for the construction of vertical sections are depicted in Figure 2.2. Temperature-salinity (T/S) transects are oriented as noted, with temperature values (°C) represented as solid lines and salinity values (Practical Salinity

25
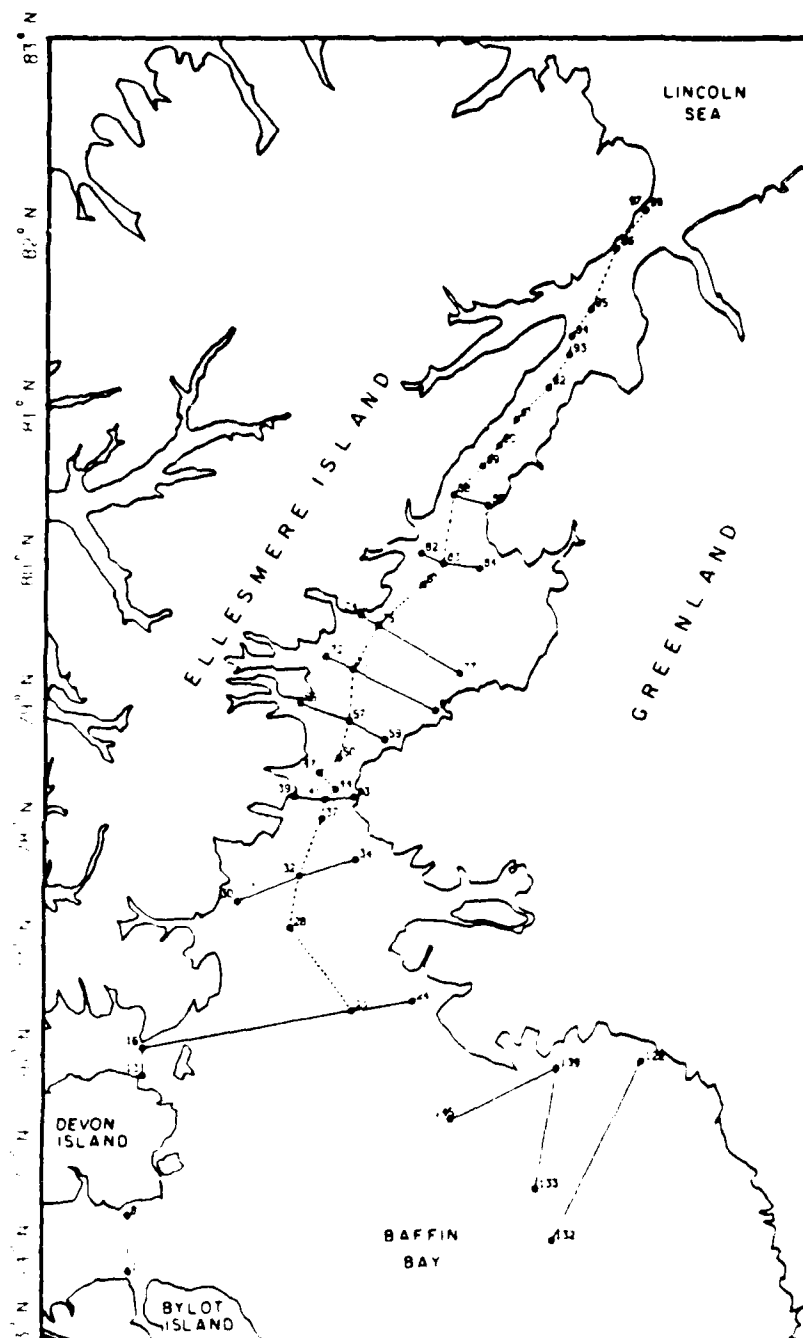
Figure 2.2   The locations of transects used in the analysis.
              The dotted line denotes stations used for
              construction of meridional cross sections.

26

Scale) represented as dashed lines. Baroclinic velocity cross sections
are oriented with velocities (cm/sec) "into" and "out of" the page
represented as solid (positive values) and dashed (negative values),
respectively.

Surface dynamic heights and baroclinic velocity profiles were
derived from the geostrophic approximation, assuming a level of no
motion of 200 dbars. The technique of Helland-Hansen (1934) was deemed
inappropriate for use in the NBB-NS region because of the inherently
shallow and irregular bathymetry, thereby precluding the selection of a
deeper reference level for regional application. Although a 200 dbar
reference level is suitable for estimating direction in near-surface
baroclinic currents, magnitudes were found to be underestimated by as
much as 25% when compared to those derived with a level of no motion of
400 dbars.

Baroclinic volume transports were calculated using variable
reference levels, determined by the maximum common sample depth in a
station pair. As the sample depths were occasionally limited by
mechanical rather than bathymetric considerations, the associated
transports may be subject to underestimation accordingly. The
transports were calculated by vertical trapezoidal integration of
baroclinic velocities over 5 m intervals.

III. **THERMOHALINE STRUCTURE**

A. INTRODUCTION

In order to more accurately characterize the near-surface and
intermediate depth waters of the NBB-NS region, a delineation of five
discrete water masses by vertical distribution of temperature and
salinity is required (Table I). Baffin Bay Surface Water (BBSW) is
derived locally and found seasonally in northern Baffin Bay at depths of
up to 75 m. It is present in both the Baffin Current and the WGC.
In general, the water masses which uniquely comprise the WGC are found
to be less saline than their counterparts which enter the NBB-NS region
through the Canadian Archipelago. Although the salinity difference
between the Polar Water fractions is small, it is useful as a
classification tool. Mixing of Arctic Basin Polar Water (ABPW) and West
Greenland Current Polar Water (WGCPW) should be expected to occur along
isopycnal surfaces in regions where their domains overlap. Although the
salinity distributions of Nares Strait Atlantic Intermediate Water
(NSAIW) and West Greenland Current Atlantic Intermediate Water (WCCAIW)
do not intersect, it is bathymetry which prevents mixing of these two
source fractions.

B. BAFFIN BAY SURFACE WATER

Baffin Bay Surface Water (BBSW) is locally derived from the combined
effects of meltwater admixture and solar heating. The large, ubiquitous
glaciers in the NBB-NS region serve as a continuous source of meltwater
during periods of insolation. Admixture of glacial runoff with Baffin
Bay Polar Water (BBPW) creates a significant halocline and resultant
pycnocline in the upper 50 m to 75 m of the water column. Concurrently,

TABLE I NEAR-SURFACE AND INTERMEDIATE DEPTH WATERS OF THE NORTHERN BAFFIN BAY-NARES STRAIT REGION

WATER MASS	CHARACTERISTICS	COMMENTS
·Baffin Bay Surface Water (BBSW)	T: > 0°C S: < 32.8 D: < 75 m	·Surface water originally defined by Coachman and Aagaard (1974) ·BBSW suggested by Fissel et al. (1982)
·Arctic Basin Polar Water (ABPW)	T: < 0°C S: < 34.8 T-S knee: 33.5 - 33.7 D: < 250 m	·Polar water originally defined by Aagaard and Coachman (1968) ·T-S knee corresponds to bottom of halocline
·West Greenland Current Polar Water (WGCPW)	T: < 0° S: < 34.2 T-S knee: 33.4 - 33.5	
·Nares Strait Atlantic Intermediate Water (NSAIW)	T: > 0°C S: 34.5 - 35.3 D: 250 m - 800 m	·AIW originally defined by Aagaard and Coachman (1968)
·West Greenland Current Atlantic Intermediate Water (WGCAIW)	T: > 0°C S: 33.8 - 34.5 D: 250 m - 800 m	·Generally warmer than NSAIW

29

the effects of solar heating are essentially confined to this surface
layer due to its inherent buoyancy. The admittedly arbitrary
delineation of BBSW by the 0°C isotherm serves to distinguish it from
BBPW, rather than imply that the effects of insolation are restricted to
a discrete temperature range. BBSW is best identified, however, by the
presence of a strong, shallow thermocline (Figure 3.1). A seasonal
reversal of the processes which create BBSW, ultimately results in its
elimination.

The distribution of BBSW is a regional phenomenon. The horizontal
distribution of maximum temperatures in the BBSW layer shows distinct
gradients in the meridional and offshore directions (Figure 3.2). This
result implies that BBSW is formed primarily by coastal processes, and
is subsequently advected throughout most of northern Baffin Bay. The
complete absence of BBSW north of Smith Sound is due to the widespread
occurrence of pack ice, which serves to raise the albedo of the region
and reduce insolation.

The considerable concentration of BBSW located in the shelf waters
of Melville Bay contributes significantly to the baroclinicity of the
WGC. A qualitative examination of a T/S transect through Melville Bay
not only indicates that a major portion of the baroclinicity occurs in
the upper 100 m, but that the isohalines (isopycnals) related to the
presence of BBSW assume a negative slope in the core of the WGC between
Stations 122 and 123 (Figure 3.3). The seasonal presence of BBSW,
therefore, would be expected to enhance the baroclinic transport of the
WGC.

30
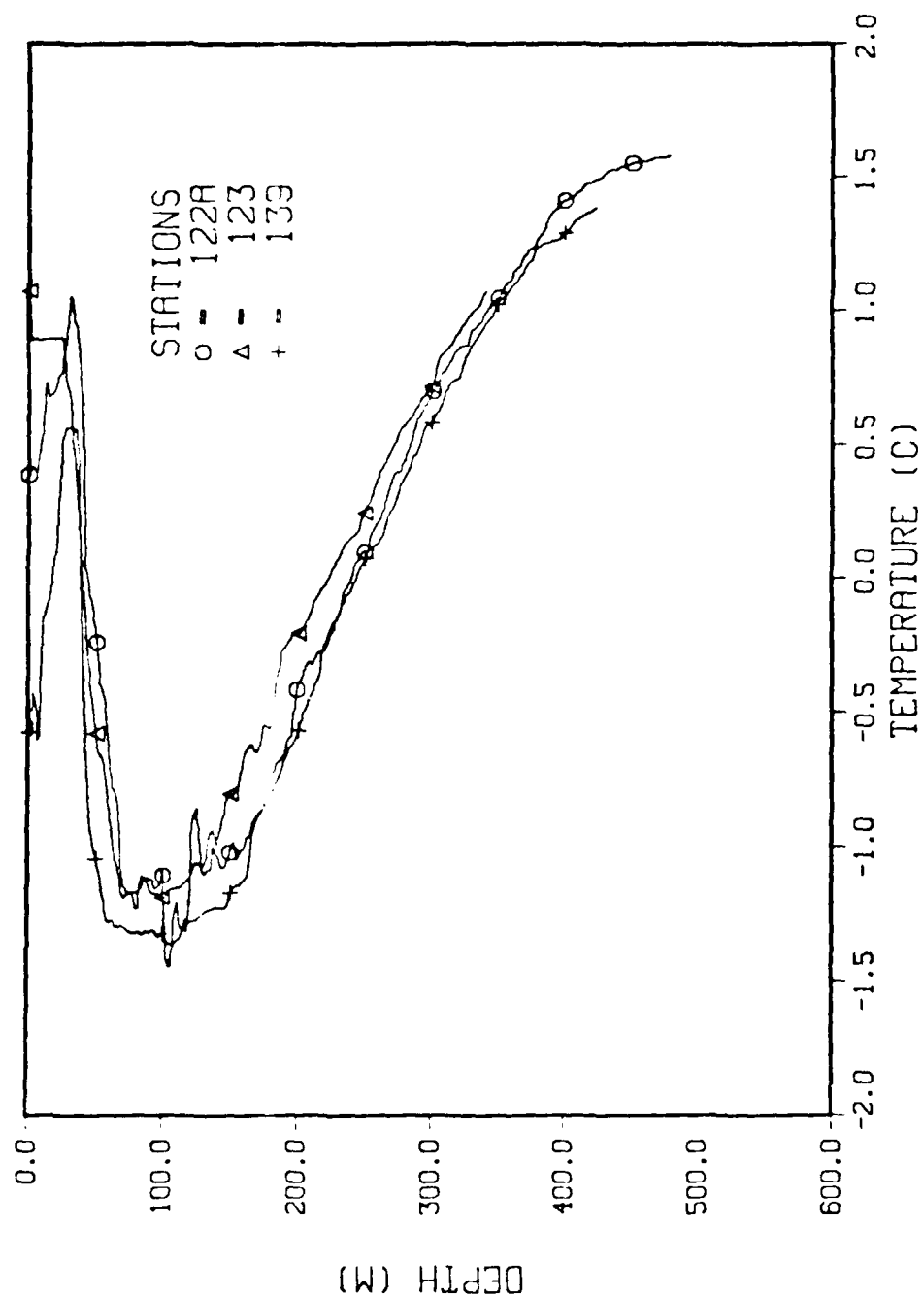
Figure 3.1   A composite temperature profile illustrating the shallow thermocline characteristic of BBSW. Refer to Figure 2.2 for station location.
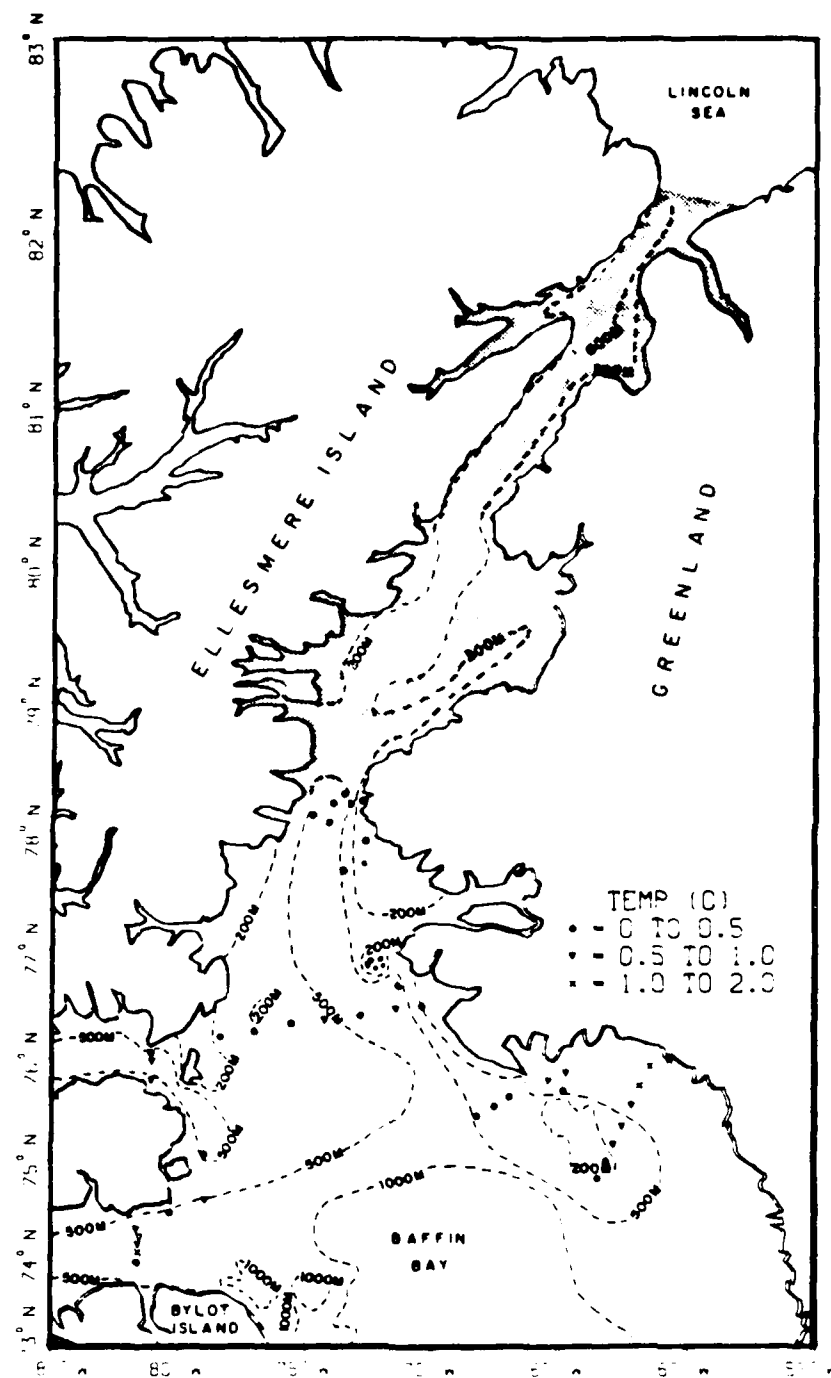
Figure 3.2   The horizontal distribution of maximum
              temperatures in the BBSW layer.
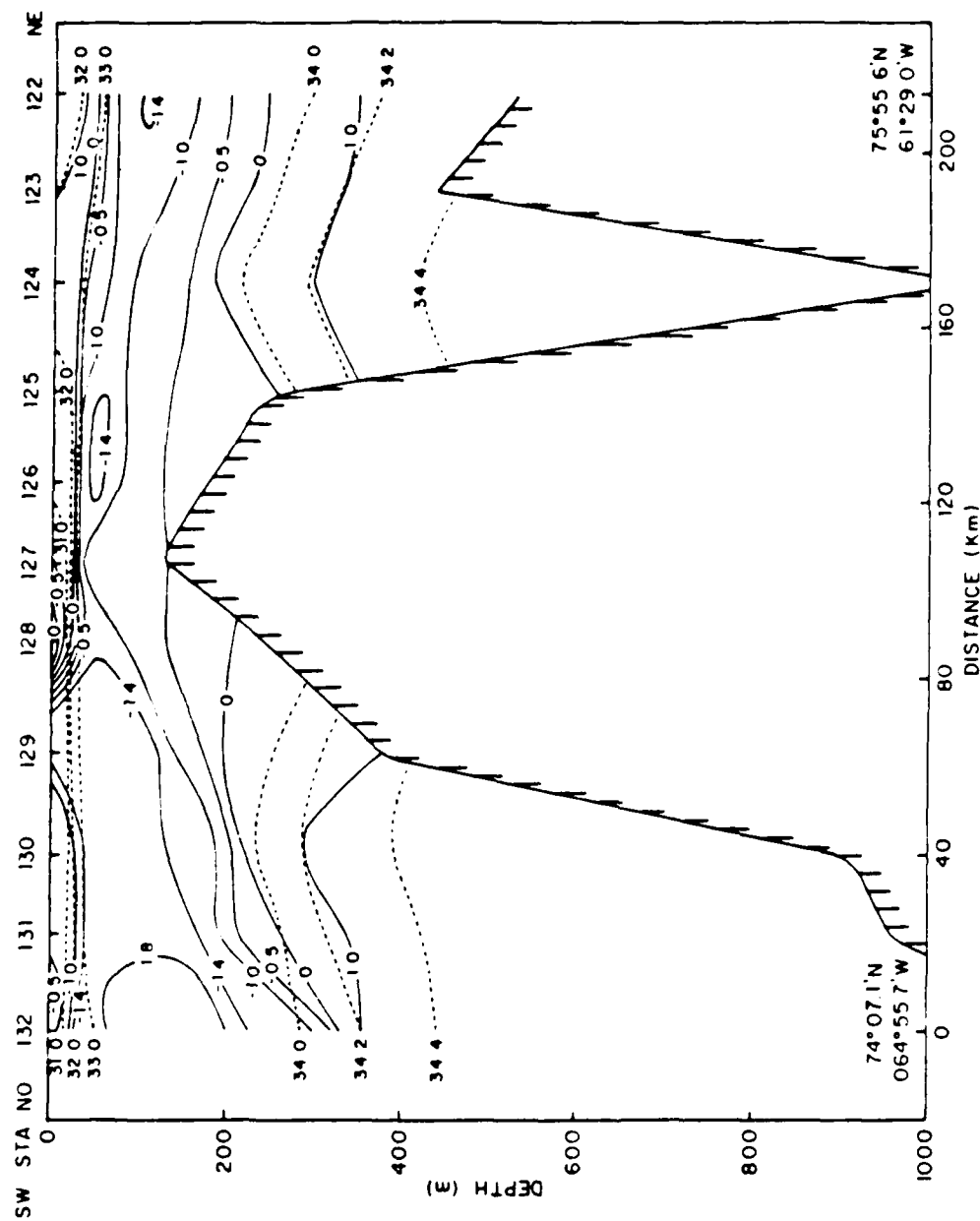
Figure 3.3   A T/S transect northeastward across Melville Bay.
Temperature contours are indicated by solid lines,
and salinity contours by dashed lines.

33

The presence of BBSW at an ice edge can be considered to represent an equilibrium state. The northernmost extent of BBSW is precisely correlated with the location of the pack ice edge. A meridional T/S transect from Baffin Bay northward to Kane Basin graphically illustrates this interaction between relatively warm surface water and an ice edge (Figure 3.4). A filament of BBSW dives subsurface between Stations 44 and 47 beneath water of lower density at the ice edge. An equilibrium state can exist if sufficient thermal advection is present to prevent ice growth. Mitigation of thermal advection or atmospheric cooling will cause the ice edge to advance or retreat, respectively.

C. POLAR WATER

Polar Water in the NBB-NS region is derived from two distinct sources. Direct inflow from the Arctic Ocean through the Canadian Archipelago is generically classified as Arctic Basin Polar Water (ABPW), whereas northward flow via the WGC through Davis Strait is termed West Greenland Current Polar Water (WGCPW). Subtle contrasts in the thermohaline signatures of these two water masses are indicative of their different origins, and serve as qualitative tracers of their respective flow fields.

Although both forms of Polar Water have origins in the Arctic Ocean, the flow of WGCPW follows a circuitous route around the southern tip of Greenland before entering the NBB-NS region. The cumulative influence of shelf and surface-driven processes on the thermohaline structure of WGCPW is, therefore, of greater magnitude than the effect of similar processes on ABPW. The primary modification which occurs is due to meltwater admixture, resulting in a net dilution of the water column.

34

Figure 3.4   A meridional T/S transect from Baffin Bay northward to Kane Basin.

Viewed simplistically, WGCPW can be considered a diluted form of ABPW.
The comparative decrease in salinity and, hence, density of WGCPW below
the surface layer is most apparent in vertical property profiles
(Figures 3.5 and 3.6). The maximum salinity of WGCPW is approximately
34.2, while ABPW reaches 34.8.

The presence of Polar Water with an underlying warm layer produces
a characteristic inflection, or knee, when temperature is plotted
against salinity. This knee can be viewed as a boundary between the
bottom of the arctic halocline, formed as a consequence of convective
overturn in winter, and a deeper thermocline, which marks the transition
to an underlying warm layer. The salinity and depth at which this knee
occurs are functions of the inherent thermohaline characteristics of the
particular Polar Water mass. The combination of relatively dilute WGCPW
and underlying Atlantic Intermediate Water results in a knee with a
salinity of 33.4 to 33.5, at depths ranging typically from 50 m to 120
m. As ABPW enters the NBB-NS region through Lancaster Sound, for
instance it is subject to interleaving and mixing along isopycnal
surfaces. This comparatively undiluted inflow is characteristically
more dense than the resident Polar Water of northern Baffin Bay, and
consequently sinks. The resultant combination of comparatively saline
ABPW and underlying Atlantic Intermediate Water produces a knee with
salinities between 33.5 and 33.7, at depths of up to 250 m. A composite
T/S curve illustrates the contrasting knee salinity ranges of WGCPW and
ABPW (Figure 3.7).

A reduction in significant insolation in the near-surface layer, or
the absence an underlying warm layer, will result in a weaker thermal
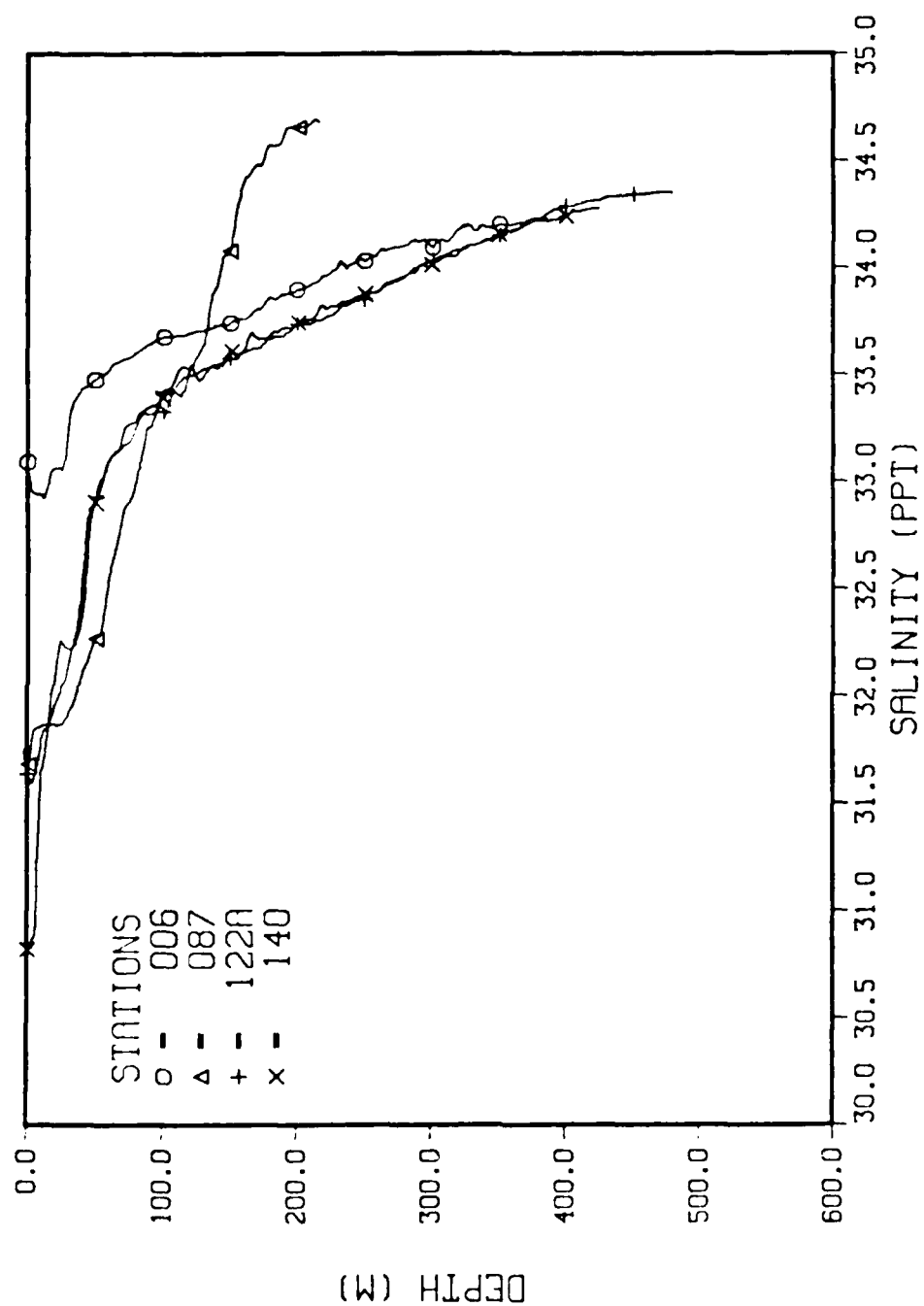
Figure 3.5 A composite salinity profile illustrating the dilution of WCCPW (Stations 122 and 140) relative to ABFW (Stations 6 and 87).

37
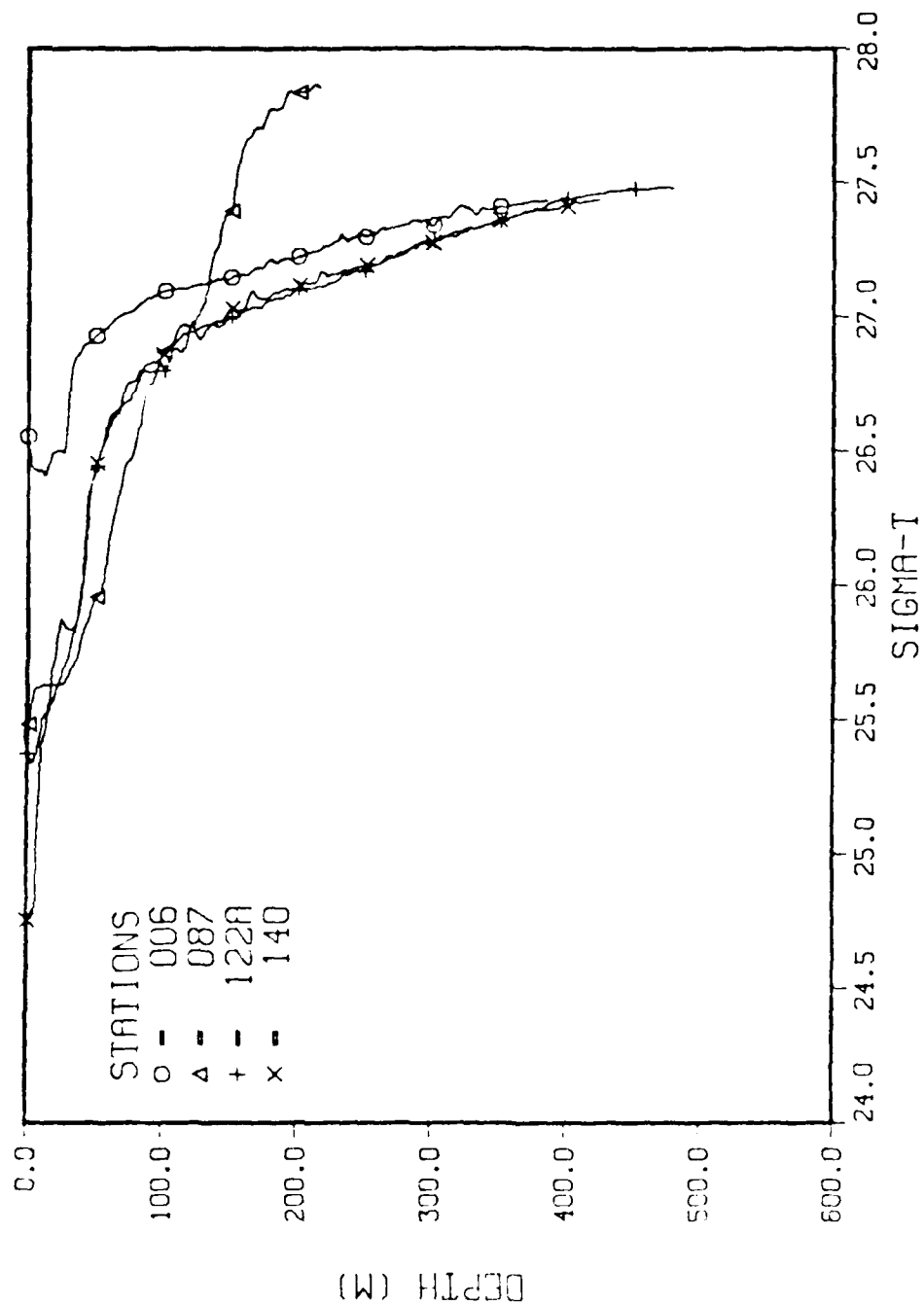
Figure 3.6   A composite density profile illustrating the
dilution of WGCPW (Stations 122 and 140) relative to
ARPW (Stations 6 and 87).

18
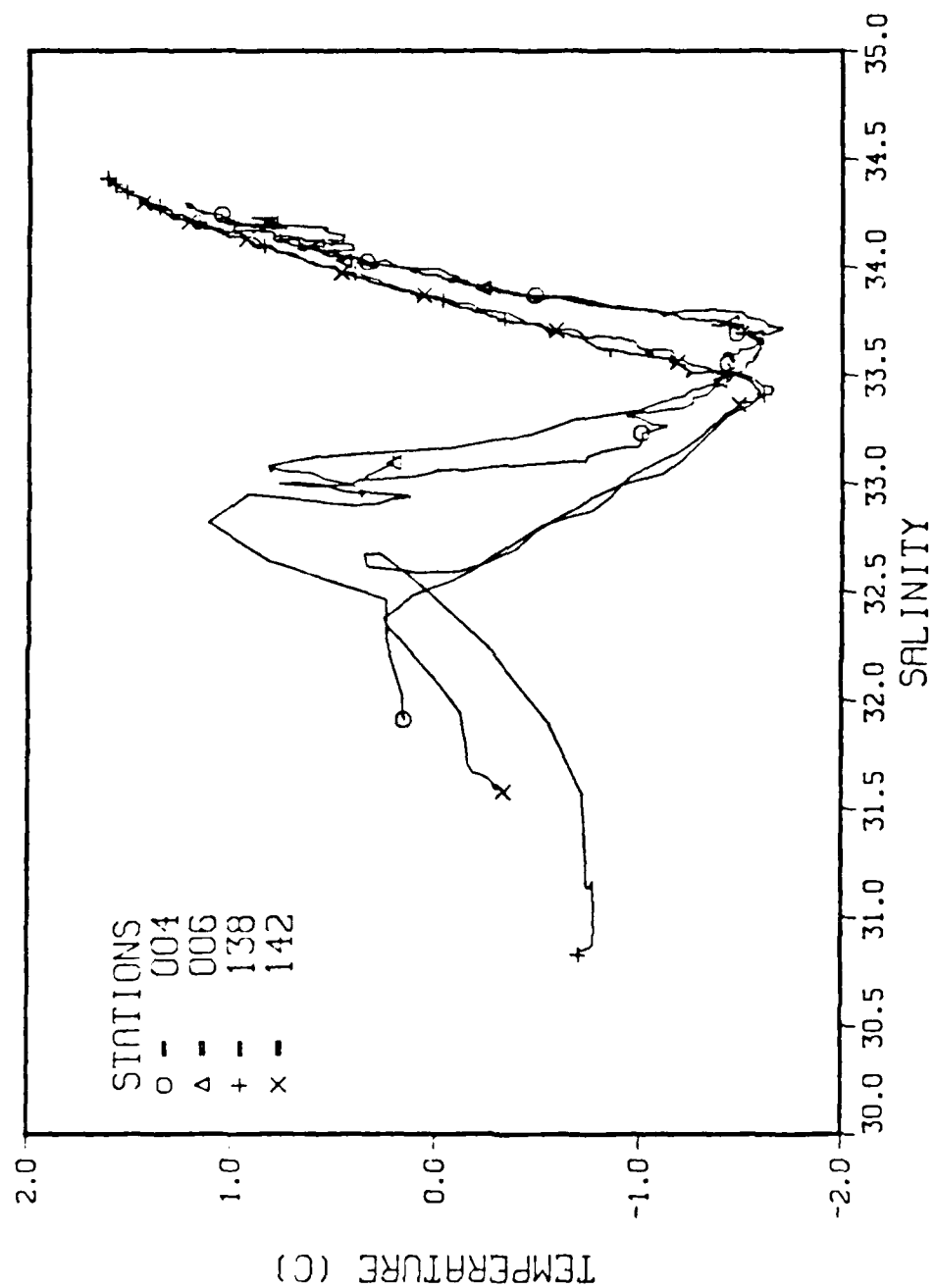
Figure 3.7   A composite T/S curve illustrating knee salinities
characteristic of WGCPW (Stations 138 and 142), and
ABPW (Stations 4 and 6).

39

gradient and a bend, rather than a sharply defined knee, in the curve.
This condition is apparent north of Smith Sound due to the widespread
occurrence of pack ice, with an associated increase in albedo
(Figure 3.8).

The thermohaline characteristics of the two Polar Water masses can
be used to roughly estimate the horizontal extent of their flow
regimes. A plan view of Polar Water distributions indicates that inflow
of WGCPW represents the minority fraction of Polar Water in the NBB-NS
region (Figure 3.9). WGCPW is prevalent along the West Coast of
Greenland northward to Cape York, where a bifurcation in flow creates
one filament which extends to Smith Sound and another which projects
westward into Jones Sound. Northward passage of WGCPW into Kane Basin
was not observed.

ABPW is present from the Lincoln Sea to the southern end of Kane
Basin, and throughout the central and western portions of Baffin Bay.
The presence of ABPW at stations north of 77°N not only suggests that
Smith Sound is a mixing site for the two Polar Water masses, but is
indicative of southward passage of ABPW from Nares Strait into northern
Baffin Bay. Inflow of ABPW is restricted to the southernmost portion of
Jones Sound, implying significant mixing there as well. Inflow of ABPW
to the region is greatest in Lancaster Sound, as indicated by the
consistently high knee salinities encountered there. A filament of
ABPW can be seen in the southwestern corner of Melville Bay at Stations
132 and 133, which marks the location of a frontal boundary between an
extreme northeastern branch of the Baffin Current, possibly derived from
Lancaster Sound outflow, and a southward flowing branch of the WGC. The

40
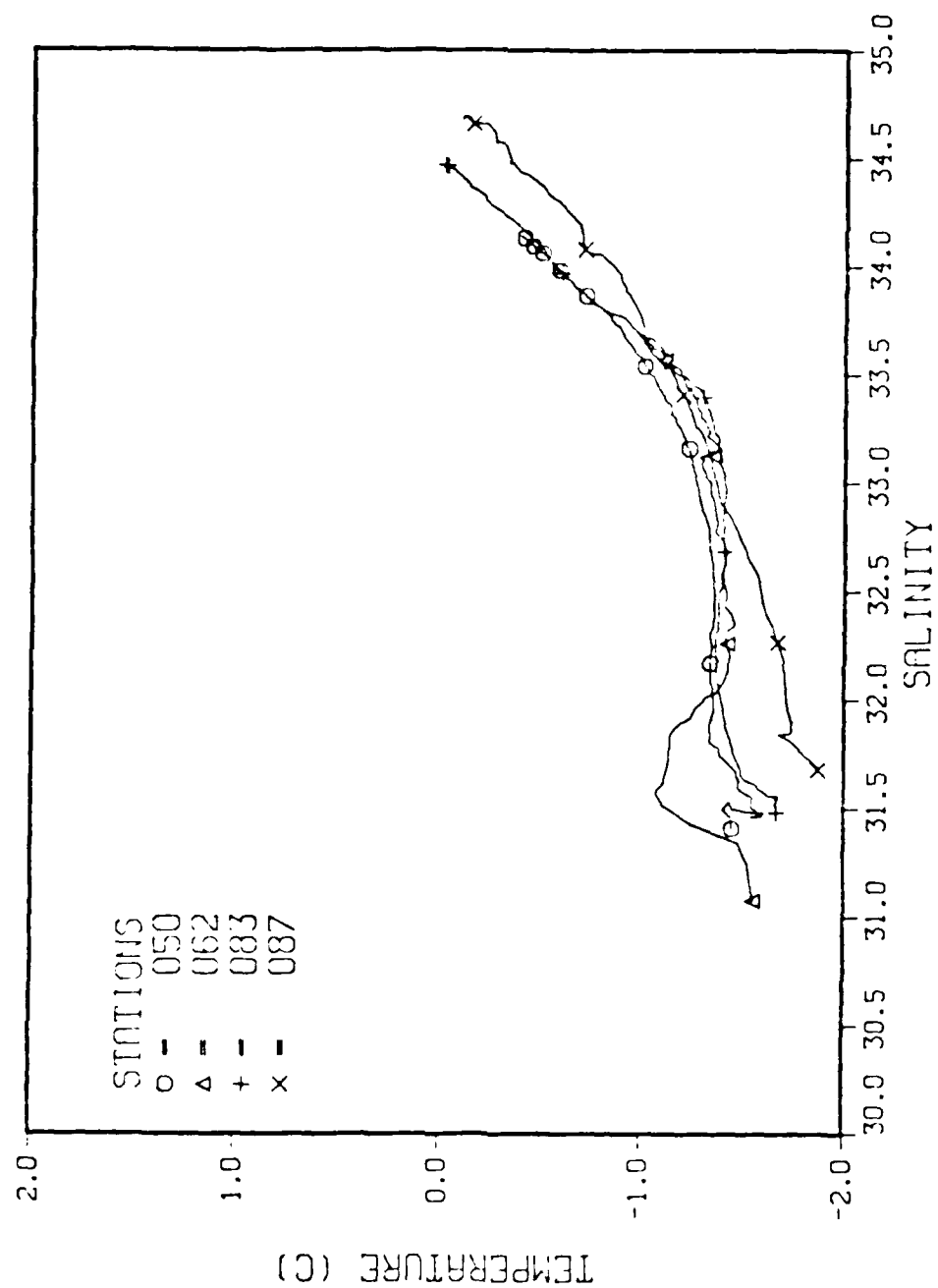
Figure 3 8 A composite T/S curve illustrating the absence of a sharp knee in stations north of Smith Sound.
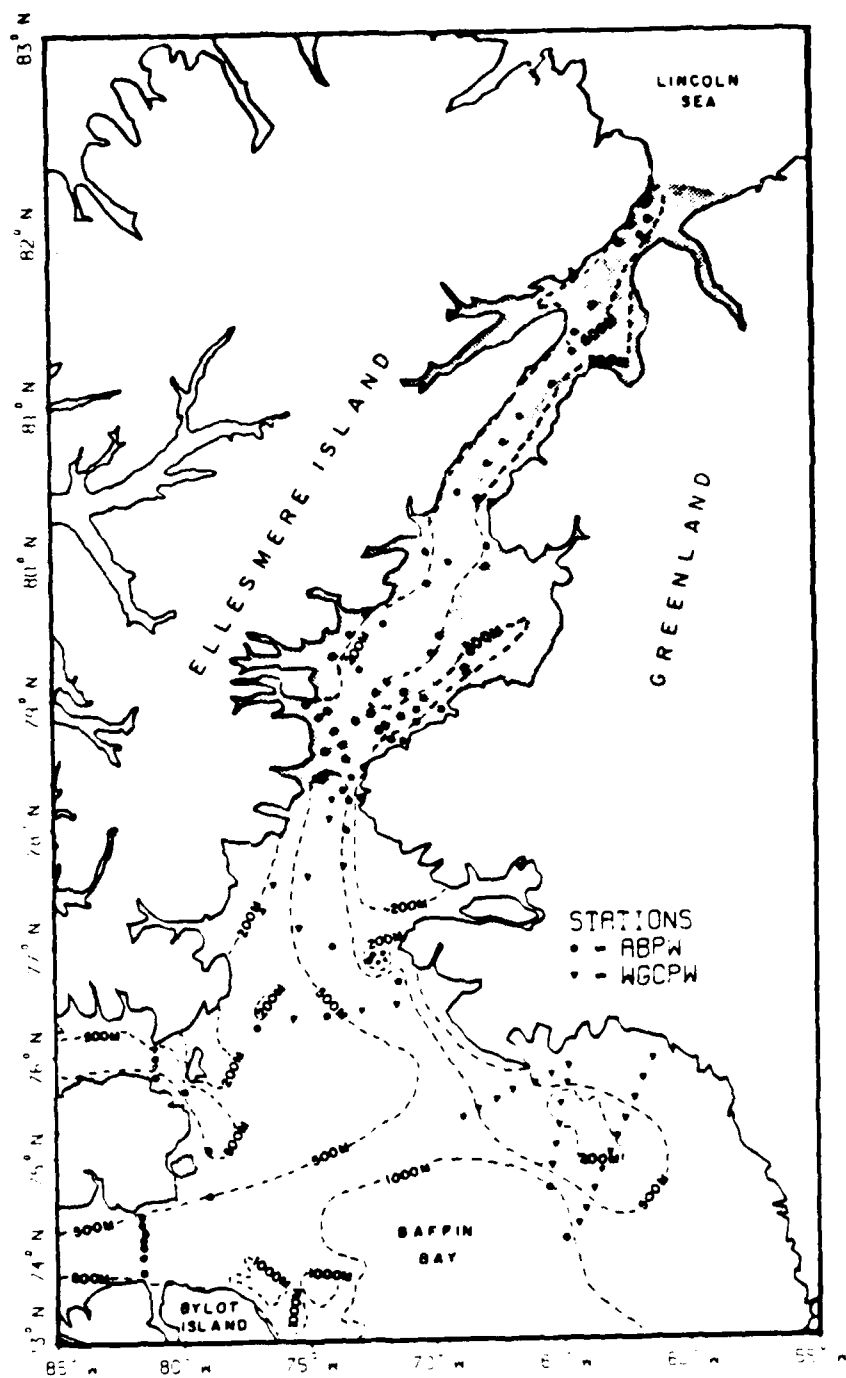
Figure 3.9   The horizontal distribution of ABPW and WGCPW in the
              NBB-NS region.

42

extensive interleaving which would be expected in regions such as these, where ABPW and WGCPW coexist, is evident in composite temperature profiles (Figure 3.10).

The presence of subsurface temperature extremes in the Polar Water layer is associated with the contrasting effects of convective overturn in winter and insolation in summer. Convective overturn during ice formation creates a cold, isohaline layer which can project to a depth of greater than 50 m locally. Lateral infusion of brine produced during the freezing of shelf waters can increase the vertical extent of this isohaline layer to over 100 m. Subsequent surface heating and meltwater mixture produces significant enthalpy increases in the shallow pycnocline layer only, isolating an underlying cold lens at depths typically between 50 m and 150 m.

South of Smith Sound cold lenses are sharply defined by strong temperature gradients. This is typically the case in Melville Bay, where cold, isohaline water is sandwiched between an overlying layer of BBSW and an underlying layer of Atlantic Intermediate Water (Figure 3.11).

The absence of cold lenses north of Smith Sound is indicative of the inherently persistent ice cover. The associated high albedo results in steadily decreasing temperatures towards the surface and, consequently, no subsurface cold lenses are apparent north of Station 72, located at approximately 79.2°N (Figure 3.12).

Southward decreases in ice concentration result in the formation of diffuse cold lenses in northern Smith Sound. A T/S transect taken at the southern entrance to Kane Basin reveals the remnants of a subsurface
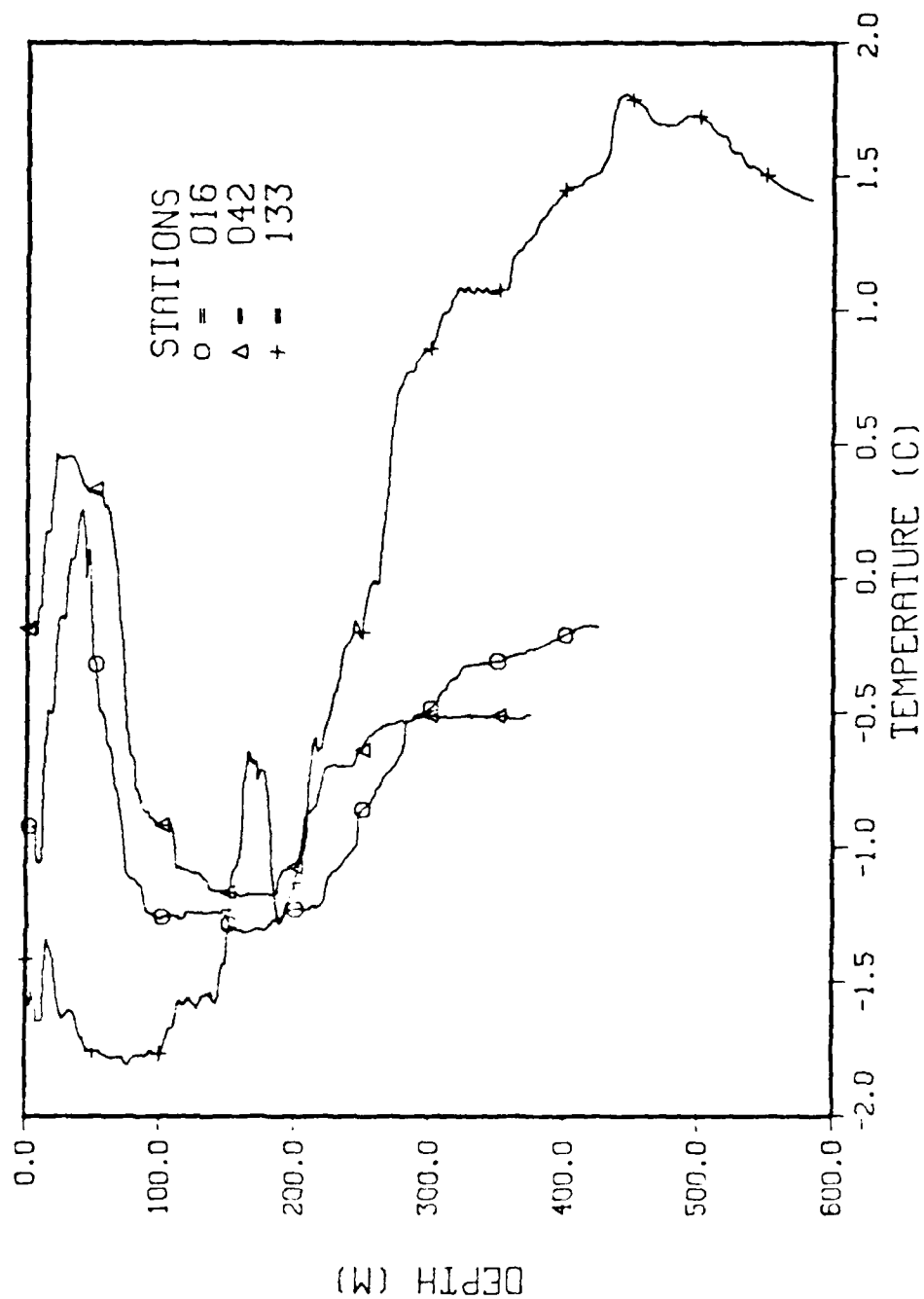
Figure 3.10   A composite temperature profile illustrating the
interleaving of ABPW and WCPW in Smith Sound
(Station 42), Jones Sound (Station 16), and Melville
Bay (Station 133).

4.

Figure 3.11   A T/S transect northward across Melville Bay.
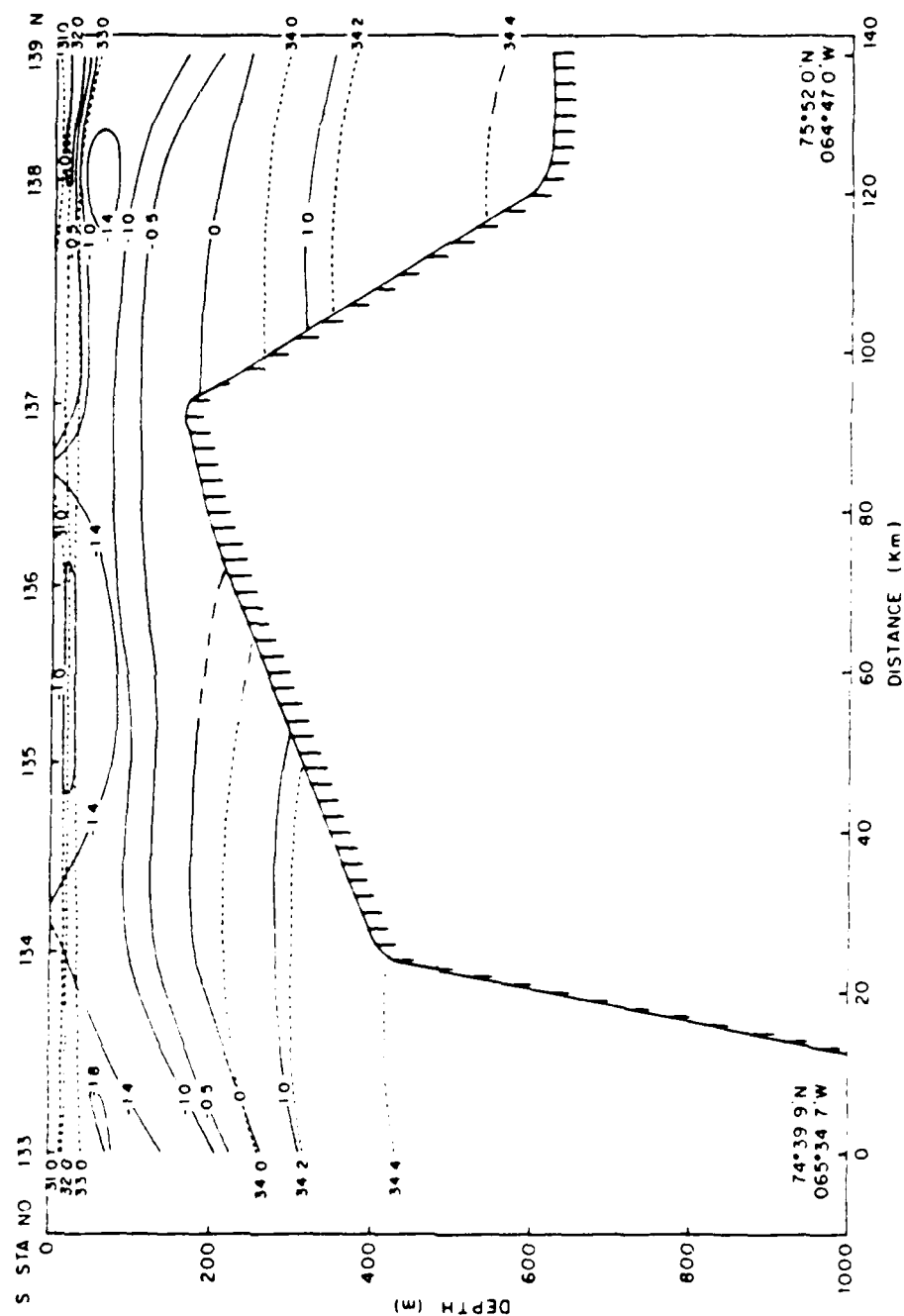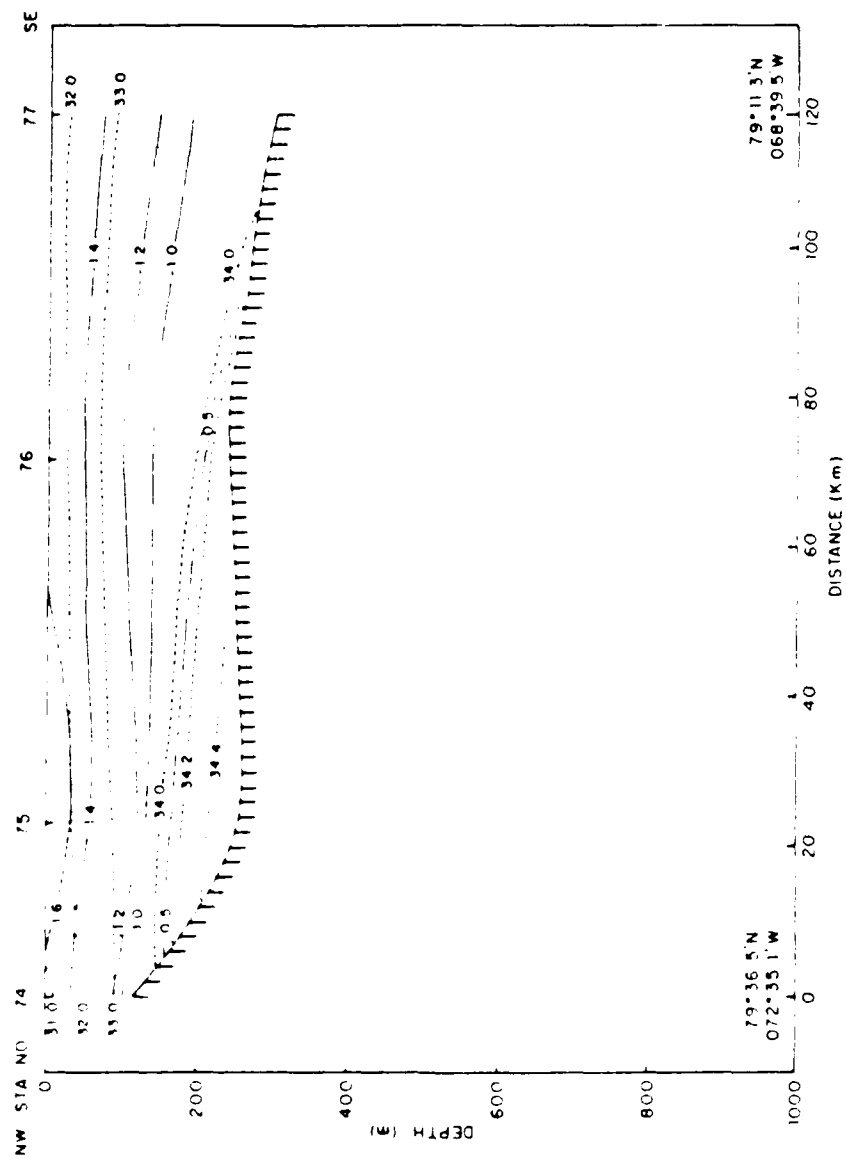
Figure 3.12   A T/S transect across Kane Basin.   Note the absence of a subsurface cold lens.

46

cold lens on the western side, and alternating warm and cold layers to the east (Figure 3.13).

Pronounced warm lenses are located on the southern side of Lancaster Sound, and along both boundaries of Jones Sound. Conditions in Jones Sound, with ambient air temperatures averaging -4°C and the presence of new ice observed along both shores, indicate that the local occurrence of subsurface lenses of BBSW is due to the initiation of convective overturn (Figure 3.14). The warm lens in southern Lancaster Sound is a sharply defined feature located at a depth of approximately 10 m (Figure 3.15). The depth of this warm lens indicates that it is probably an outflow jet of ABPW which dives subsurface upon encountering a cooler, but comparatively less saline layer of resident Polar Water. This effect further illustrates the point that ABPW is more saline than the residual Polar Water mixture of northern Baffin Bay, and is subject to mixing along isopycnals at deeper depths.

The major source of meltwater in the NBB-NS region is the Humboldt Glacier, located on the eastern side of Kane Basin. All stations in Kane Basin south of approximately 79°56'N (Station 84) have low surface salinities, typically approaching 31.0, and exhibit significant stair-stepped layering in vertical density structure (Figure 3.16). This not only illustrates the magnitude of glacial influence in the region, but suggests that extensive recirculation of near-surface waters may occur in Kane Basin. A significant local source of meltwater is apparent in the northwest corner of Robeson Channel, where surface salinities were generally below 30.0, the lowest encountered in the NBB-NS region (Figure 3.17).

47
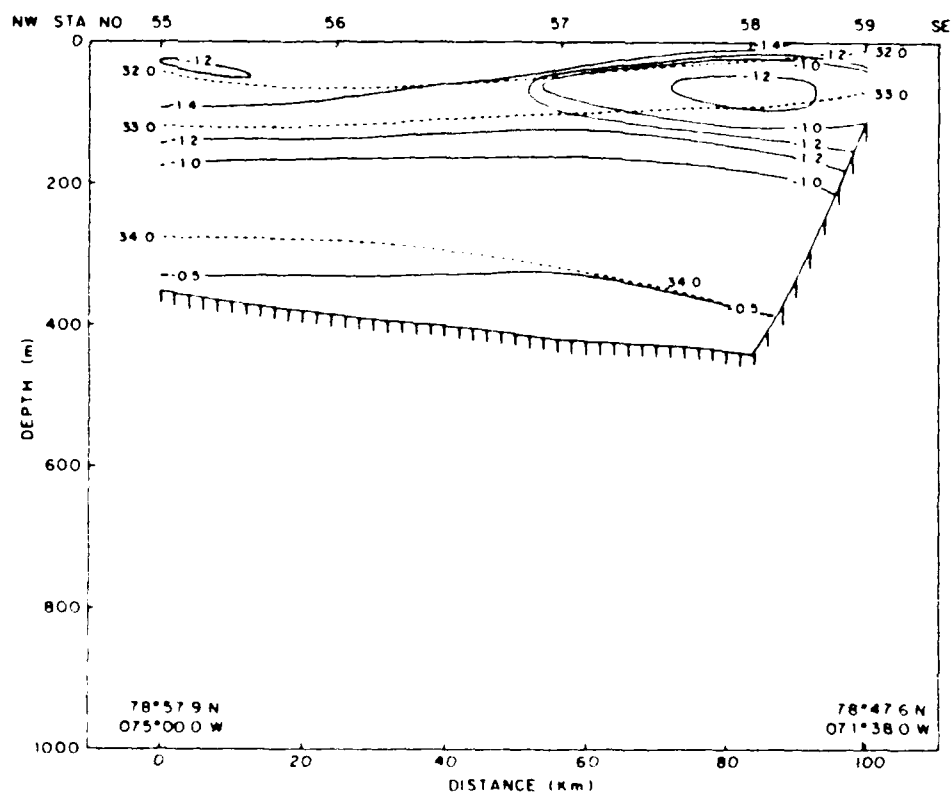
Figure 3.13   A T/S transect across the southern entrance to Kane
                Basin. Note the remnant of a cold lens at Station
                55, and alternating warm and cold layers to the
                east.

48
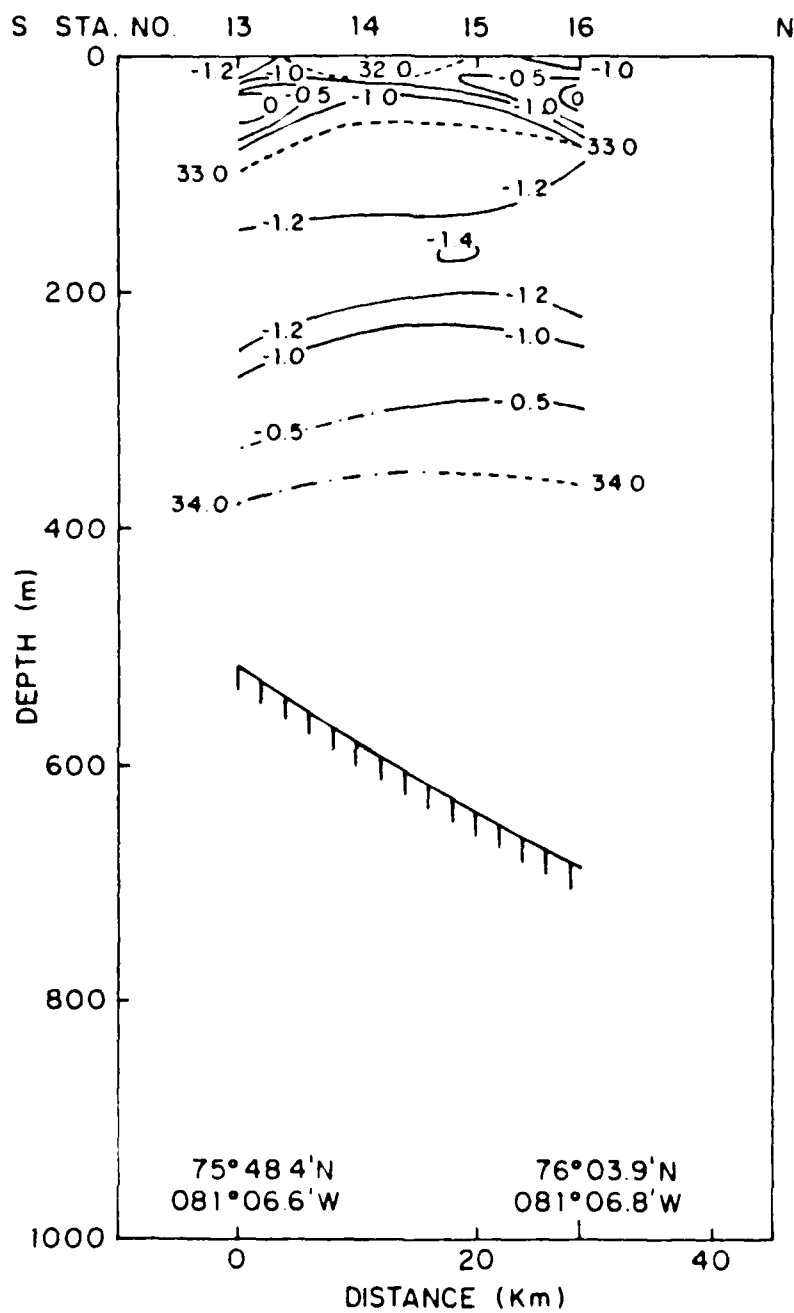
Figure 3.14   A T/S transect across the mouth of Jones Sound.

49

Figure 3.15   A T/S transect across the mouth of Lancaster Sound.
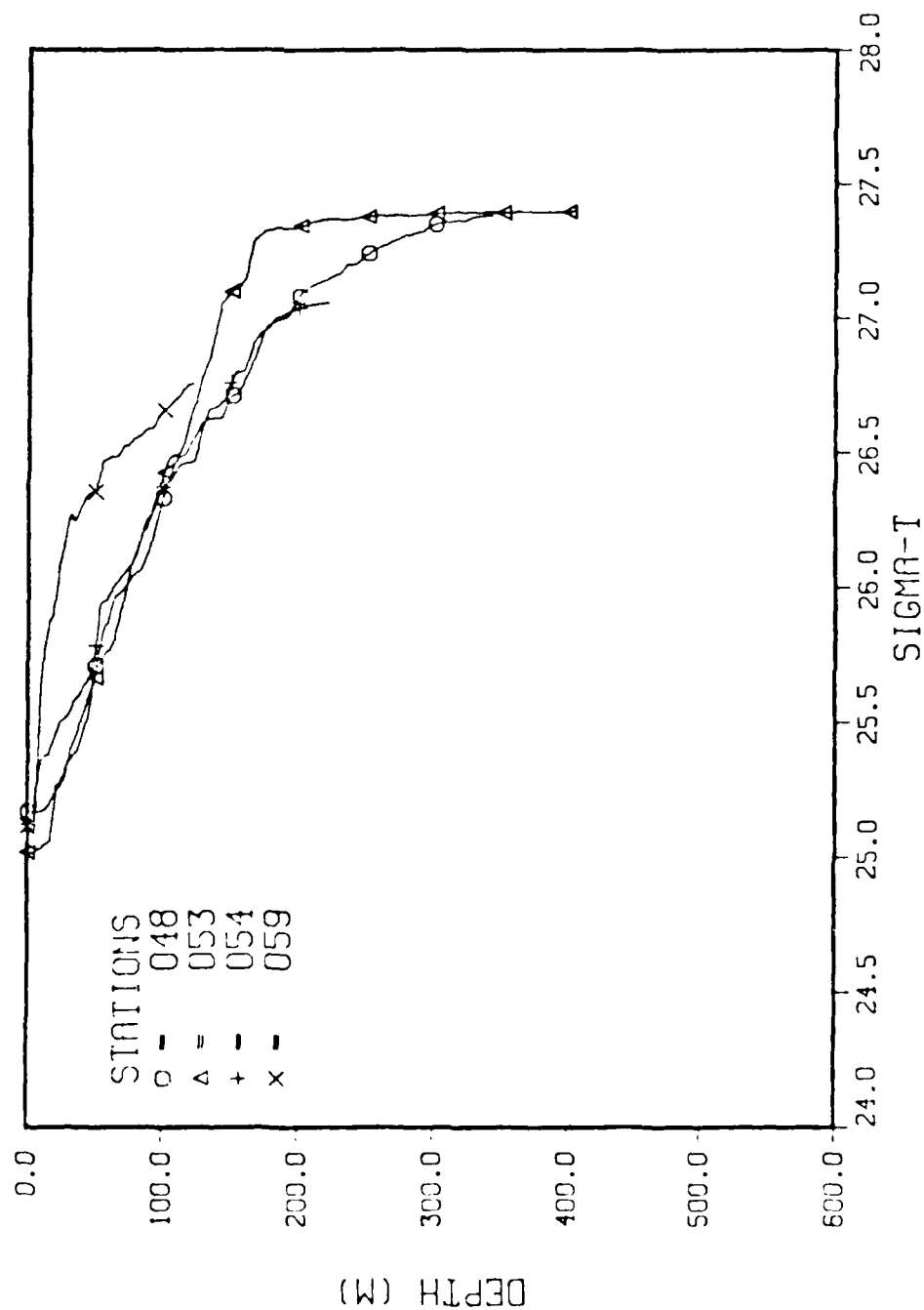
Figure 3.16   A composite density profile illustrating the magnitude of glacial meltwater-induced stair-stepped layering in Kane Basin.
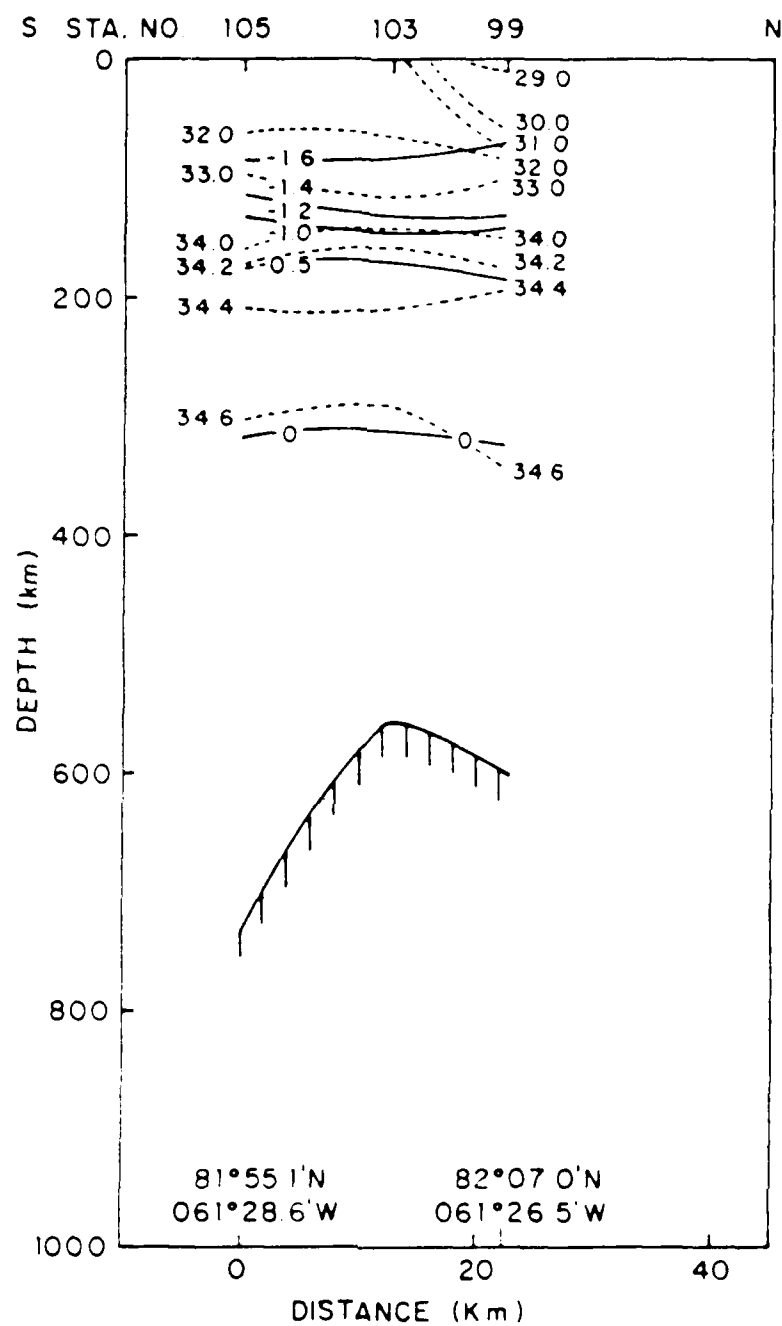
Figure 3.1   A T/S transect in Robeson Channel.

D. ATLANTIC INTERMEDIATE WATER

The two Atlantic Intermediate Water fractions found in the NBB-NS region exhibit inherently different salinity characteristics and exclusive horizontal distributions. Nares Strait Atlantic Intermediate Water (NSAIW) is derived from the Atlantic Layer of the Arctic Basin and flows southward from the Lincoln Sea into Nares Strait. West Greenland Current Atlantic Intermediate Water (WGCAIW) flows northward through eastern Davis Strait, advected by the WGC into northern Baffin Bay.

WGCAIW is warmer but less saline than NSAIW. Following the same line of reasoning which requires subdivision of the Polar Water fractions, WGCAIW is subject to more significant dilution effects by shelf and surface-driven processes compared to direct inflow from the Arctic Basin. Since CTD cast depths were not deep enough to reach the bottom of the WGCAIW layer, the upper limit in salinity presented in Table I for this water mass should be considered an estimate. The maximum salinity encountered in WGCAIW was 34.44, at a depth of 562 m (Station 124), whereas a maximum salinity of 35.24 was recorded for NSAIW at a depth of 481 m (station 97). The comparatively lower temperatures in NSAIW are a reflection of the general north-south temperature gradient in the region. The highest Atlantic Layer temperature recorded in NSAIW was $0.20°C$ at a depth of 715 m (Station 95), in contrast with a maximum temperature of $1.81°C$, recorded at a depth of 445 m (Station 133) for WGCAIW.

The horizontal distributions of NSAIW and WGCAIW in the NBB-NS region are primarily determined by depth-scale isobaric regimes. The

53
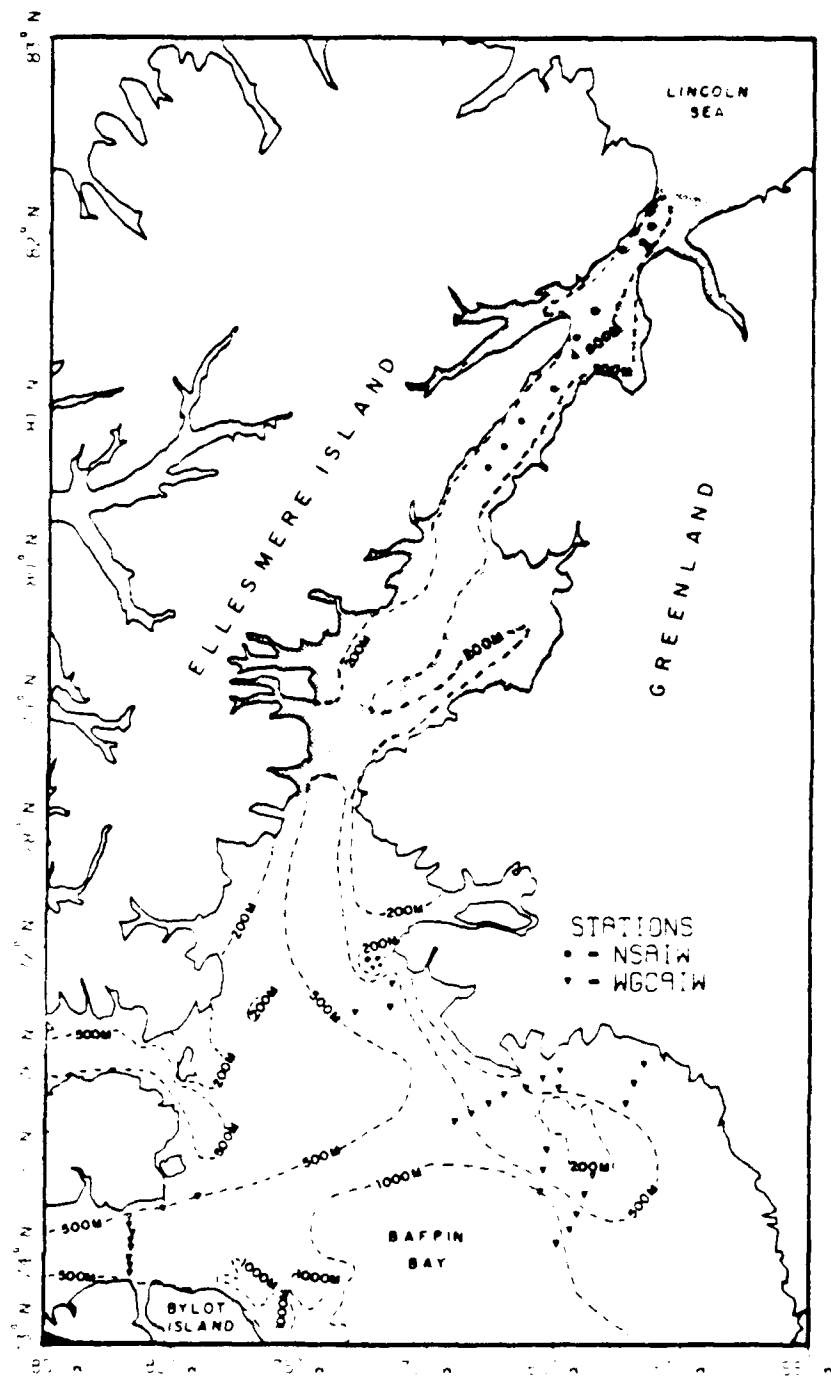
Figure 3.18   The horizontal distribution of NSAIW and WGCAIW
in the NBB-NS region.

54

Southward passage of NSAIW into Kane Basin is prevented by shoaling of the sea floor in southern Kennedy Channel (Figure 3.19). Although the major portion of WGCAIW flow is turned cyclonically to the southwest by the coastlines of Melville Bay and Cape York, northward transport of the remainder is abruptly terminated by a shallow bank (200 m) located in the vicinity of the Carey Islands. Northward flow of WGCAIW could continue to follow a deep narrow channel around this bank (Figure 3.20) but was not observed to do so. Once turned to the southwest, the flow of WGCAIW throughout northern Baffin Bay is not restricted by bathymetry. It should be noted that even with the hypothetical occurrence of westward flow from Cape York, penetration into Jones Sound by WGCAIW would be impossible because of shallow banks located east of the mouth. The flow into Lancaster Sound, however, is not similarly restricted. It is apparent that southeastern Lancaster Sound is a site of significant interleaving of dissimilar water masses, as the associated T/S cross section reveals the presence of BBSW, ABPW, and WGCAIW in profile (refer to Figure 3.15). It is presumed that WGCAIW is present at stations 7, 8, 9, 10 and 11, although the shallow CTD casts at these stations precludes absolute confirmation.
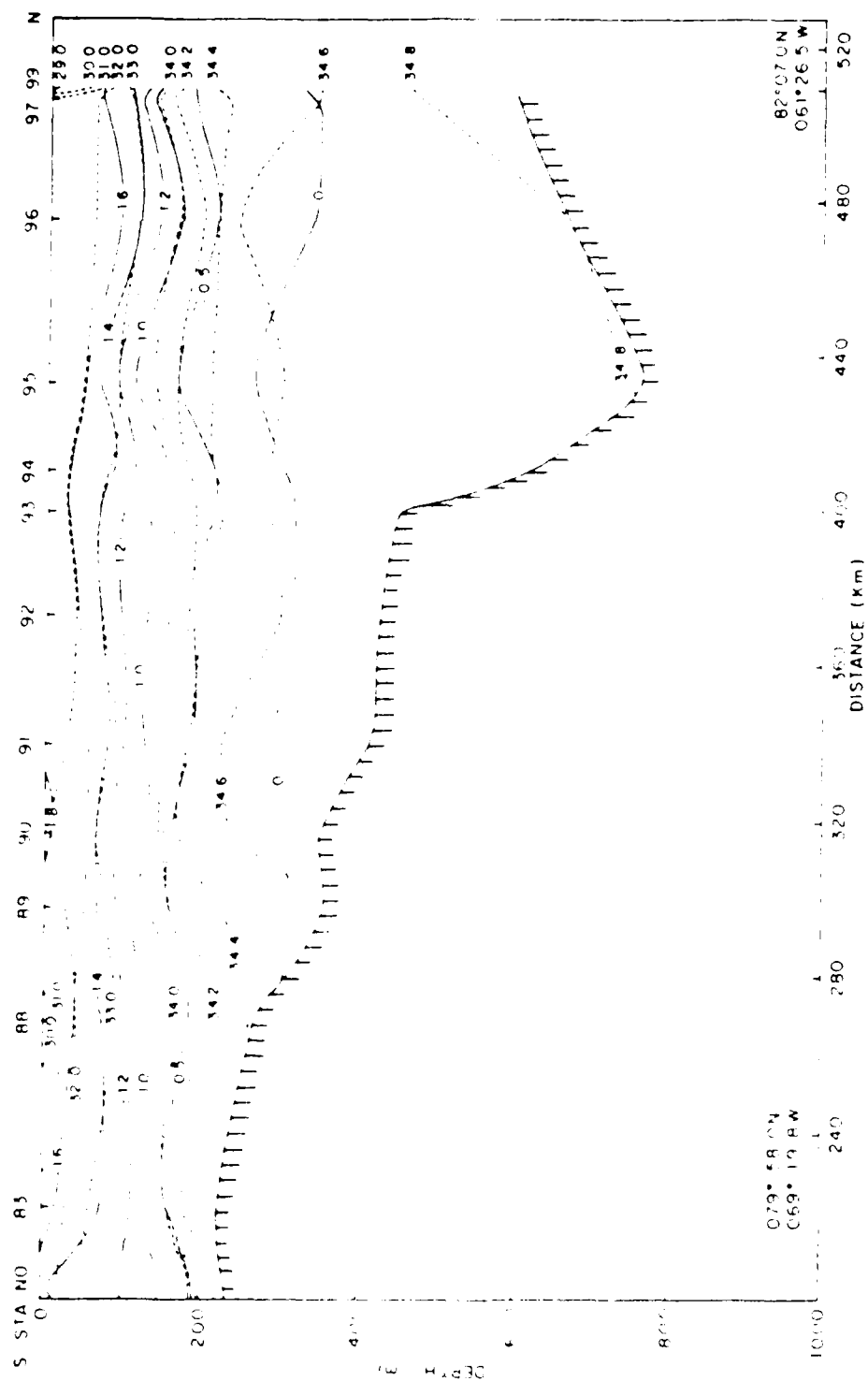
Figure 3.12 A meridional T-S transect from Kane Basin northward through Kennedy and Robeson Channels. The meridional distribution of RSAIW is indicated by the extent of the 0°C isotherm.
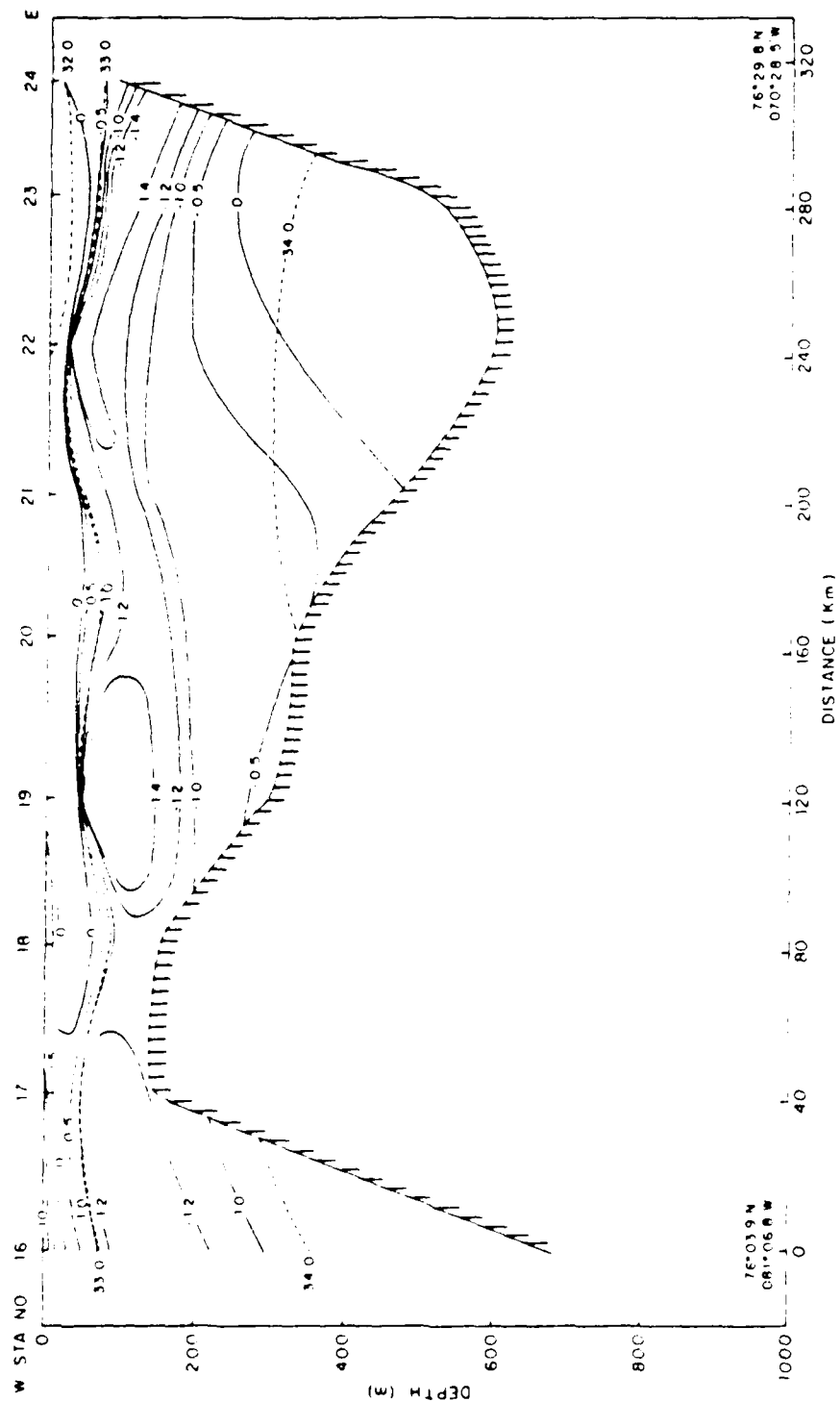
Figure 3.20   A T/S transect from Jones Sound eastward to
Thule. The flow of WGCAIW (defined by the deep
0°C isotherm) is confined to a narrow channel.

A. INTRODUCTION

Macroscale circulation in the NBB-NS region is dominated by the northward flowing WGC and the southward flowing Baffin Current. Although net southward flow in the region is maintained primarily by baroclinic forcing (Muench, 1971), bathymetry exerts considerable influence on the formation of mesoscale circulation patterns. An examination of the surface circulation of the region, as deduced from baroclinic velocity and dynamic height calculations, reveals the nature of this influence (Figure 4.1). Reference to this surface circulation diagram is implied in the ensuing discussions.

B. DYNAMIC TOPOGRAPHY

An examination of the surface dynamic topography of the NBB-NS region referenced to 200 dbars indicates a general westward increase in dynamic heights (Figure 4.2). This trend is associated with the influence of the Coriolis force on the net southward flow.

The shoreward gradient of the dynamic height contours, in northern Baffin Bay lends a cyclonic appearance to the circulation pattern. Meltwater runoff may be responsible for the increase in dynamic heights along the coastline of Melville Bay. The complex circulation patterns associated with the WGC are inferred from the reversal of gradients and bending of contours in the vicinity of Cape York. Northwestward flow around Cape York is diverted seaward, all the way in the vicinity of the Carey Islands, and north is associated with the separation of southward flow and the influence of the branch of the WGC that partially rejoins Melville Bay. The flow reversal occurs on
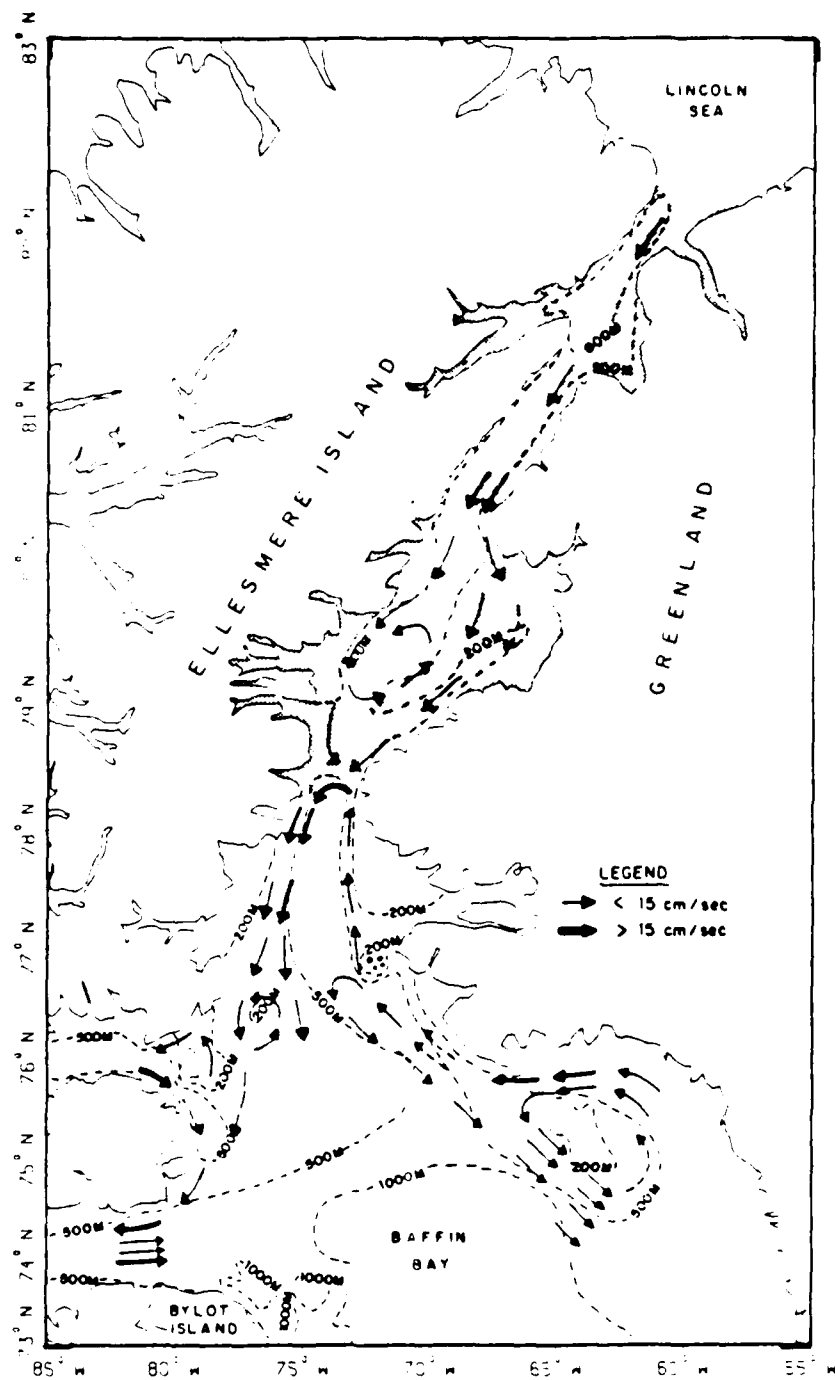
Figure 4.1   Surface circulation in the NBB-NS region as deduced from
baroclinic velocity and dynamic height calculations.
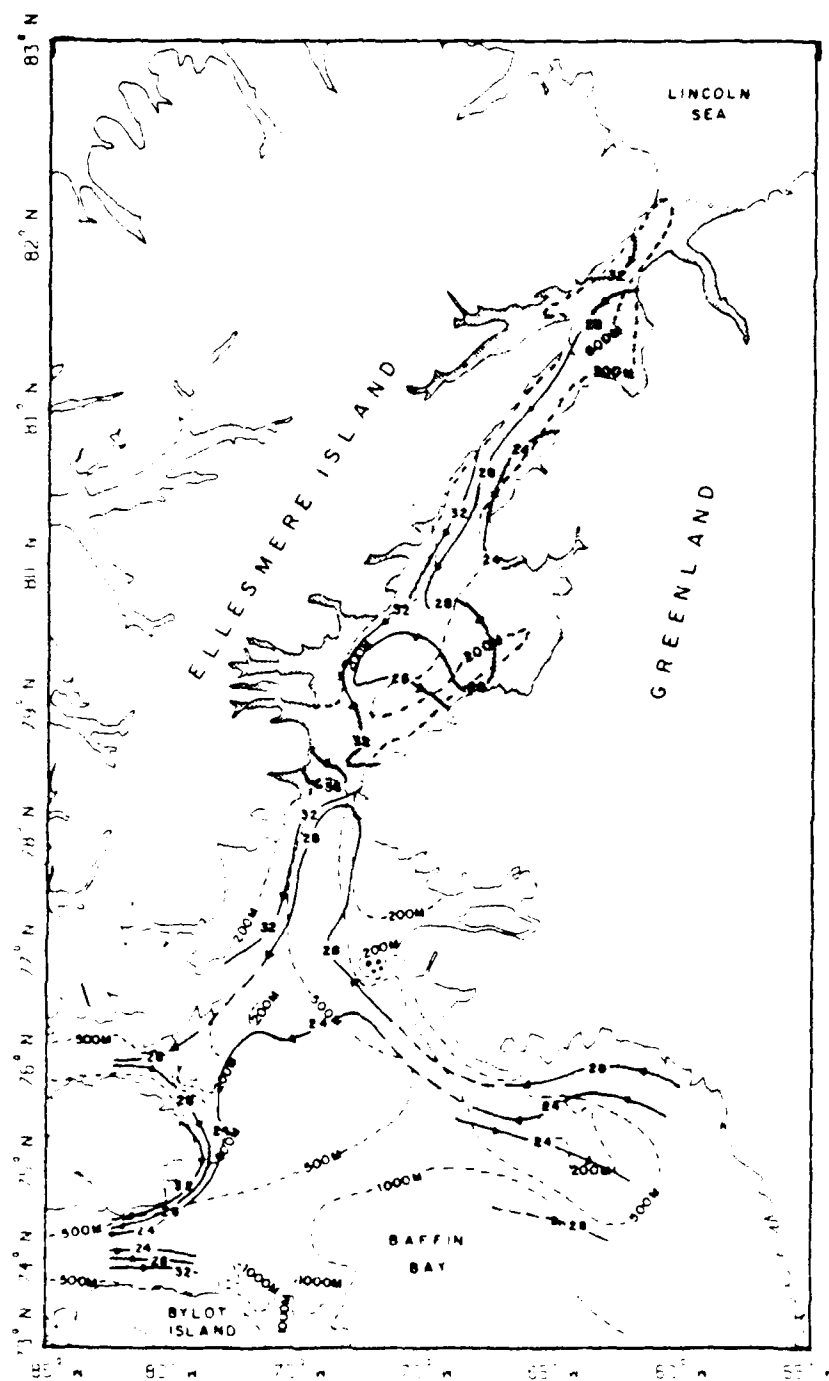
Figure 4.2   The surface dynamic topography referenced to 200
             decibars, in dynamic centimeters.

60

the perimeter of a shallow bank, suggesting a possible topographic influence. Westward intrusions of surface flow are apparent at the northern sides of the entrances to both Lancaster and Jones Sounds. Although net flow is eastward in both cases, the closer spacing of contours in Lancaster Sound is associated with much greater baroclinic velocities. A significant portion of the ABPW outflow from Jones Sound into northern Baffin Bay is turned anticyclonically around the southeast shore of Devon Island, augmenting the westward intrusion of flow into Lancaster Sound.

The sharp bending of contours in Smith Sound marks the boundary between two intersecting circulation regimes. A northward flowing branch of the WGC turns cyclonically, coincident with the formation of an ice-edge jet at the southern limit of the ice pack. The 0.36 dynamic meter contour is representative of the impingement of the relatively warm surface current on the ice pack, with a resultant density gradient normal to the ice edge. The deflection of southward flow from Nares Strait at the front is also apparent, but determination of associated circulation patterns within Kane Basin is not possible at this resolution. The meandering 0.28 dynamic meter contour in Kane Basin, however, is suggestive of the potential for gyre formation in this region.

C. THE WEST GREENLAND CURRENT

Circulation of the WGC in northern Baffin Bay appears to be governed by conservation of potential vorticity. As a typical eastern boundary current, the WGC may be assumed to have a substantial barotropic component of flow. Conservation of potential vorticity

requires barotropic flow to follow lines of constant f H, where f is the Coriolis parameter, and H is the water depth. Since mesoscale variations in the Coriolis parameter can be considered negligible, flow will tend to parallel isobaths.

Justification of the preceeding assumptions in the case of the WGC is provided by a number of observations. Although the direction of mean flow in the WGC is closely correlated with the 500 m isobath, recurvature to the west and south is noted at three primary locations. In Melville Bay the flow is observed to recurve southeastward around a shallow bank. A cross section of baroclinic velocities in this area not only indicates significant deep flow around the periphery of the bank, but confirms the filamental nature of the return current (Figure 4.3). The two distinct flow regimes on the southwest side of the bank are, as stated in Chapter 3, of different origins. Flow between Stations 128 and 129 is a recurved branch of the WGC which, assuming conservation of relative vorticity, probably forms a cyclonic gyre around the perimeter of the bank. Southwest of an apparent frontal boundary, however, a second axis of flow exists which has been shown to principally contain ABPW.

Shoaling of the bottom in the vicinity of the Carey Islands causes complete recurvature of WGCAIW. The baroclinic velocity cross section from Jones Sound westward to Thule reveals that the core of the WGC is found east of Station 22 (Figure 4.4). Since water of Atlantic layer origin has been confirmed between Stations 21 and 24, recurved flow of WGCAIW must pass between Stations 21 and 24. A depiction of baroclinic velocities between Stations 21 and 24 shows the recurved motion occurred
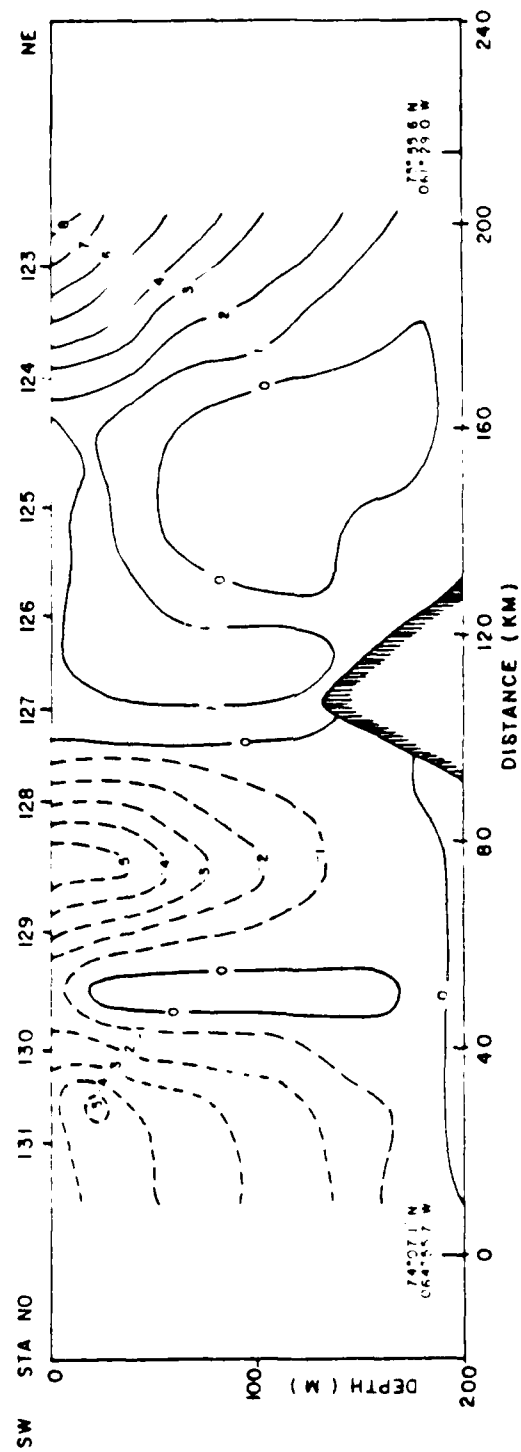
Figure 4.3 A baroclinic velocity cross section through Melville Bay. Velocities between successive station pairs were derived from the geostrophic approximation, assuming a level of no motion at 200 dbars. Northward flow is indicated by positive isotachs, and southward flow by negative isotachs.

63
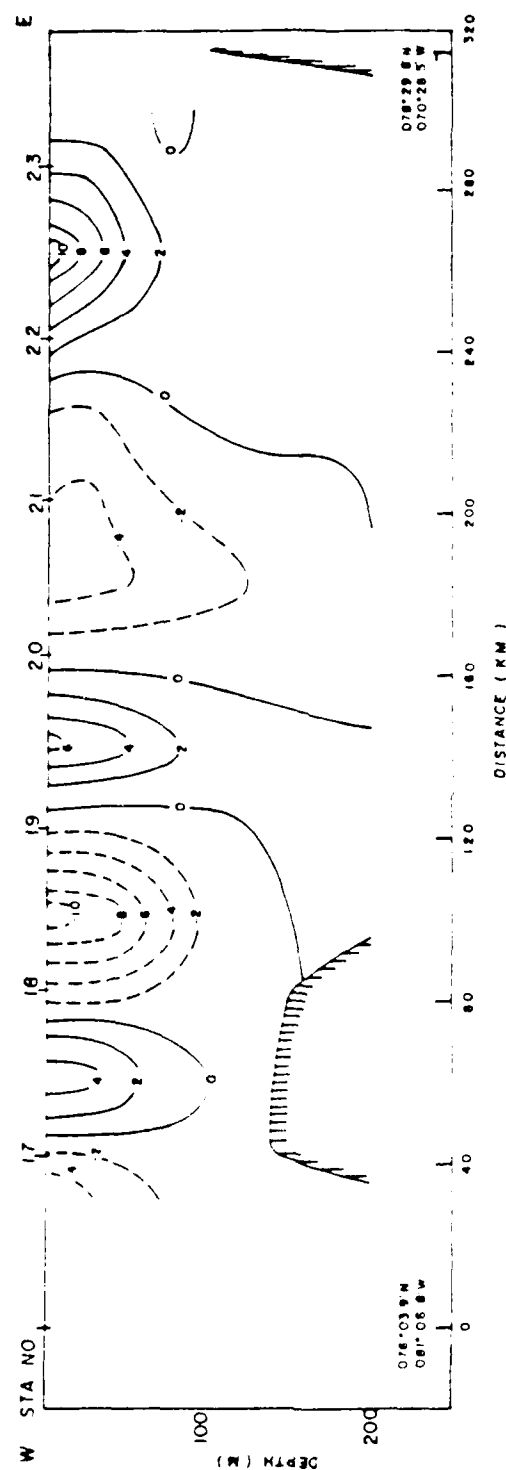
Figure 4.4 A baroclinic velocity cross section from Jones Sound eastward to Thule. The main cores of the Baffin Current and the WGC are located between Stations 18 and 19, and Stations 22 and 23, respectively. The axes of flow for topographically-influenced cyclonic gyres associated with Coburg Island (not visible) and the 150 m bank are located at Stations 17 and 19, respectively.

64

at 375 m, indicates that southward flow for this station pair is limited
to the upper 55 m of the water column. Northward flow between
Stations 22 and 23, calculated with a level of no motion at 400 m,
decreased from 0.12 m/s at the surface to less than 0.03 m s at a depth
of 115 m. The implication of this result is that most baroclinicity in
the WGC is confined to the surface and near-surface layers. Barotropic
currents are presumed to dominate below this level, hence, the
postulated influence of topographic steering on the WGC.

The remaining branch of the WGC is recurved at the northern extent
of the 500 m isobath in Smith Sound. A meridional velocity cross
section through the region further substantiates the classification of
the baroclinic component of this flow as an ice edge jet (Figure 4.5)
Baroclinic velocities between Stations 41 and 44, calculated with a
level of no motion at 400 m, decreased from 0.44 m/s at the surface to
approximately 0.04 m/s at 200 m. Below 200 m, predominantly barotropic
flow is topographically steered to the west and south by rapid shoaling
of the bottom.

). CIRCULATION IN NARES STRAIT

The macroscale circulation regime in Nares Strait generates net
southward flow of ABPW into Smith Sound. Mesoscale circulation patterns
in the region, however, can not be characterized so succinctly.

Inflow from the Lincoln Sea proceeds southward through Robeson and
Kennedy Channels. A baroclinic velocity cross section through a
southern part of Kennedy Channel indicates the relatively uniform nature
of this flow (Figure 4.6). Recalling that southward flow of NSAIW is
terminated by rapid shoaling just north of this transect (refer to
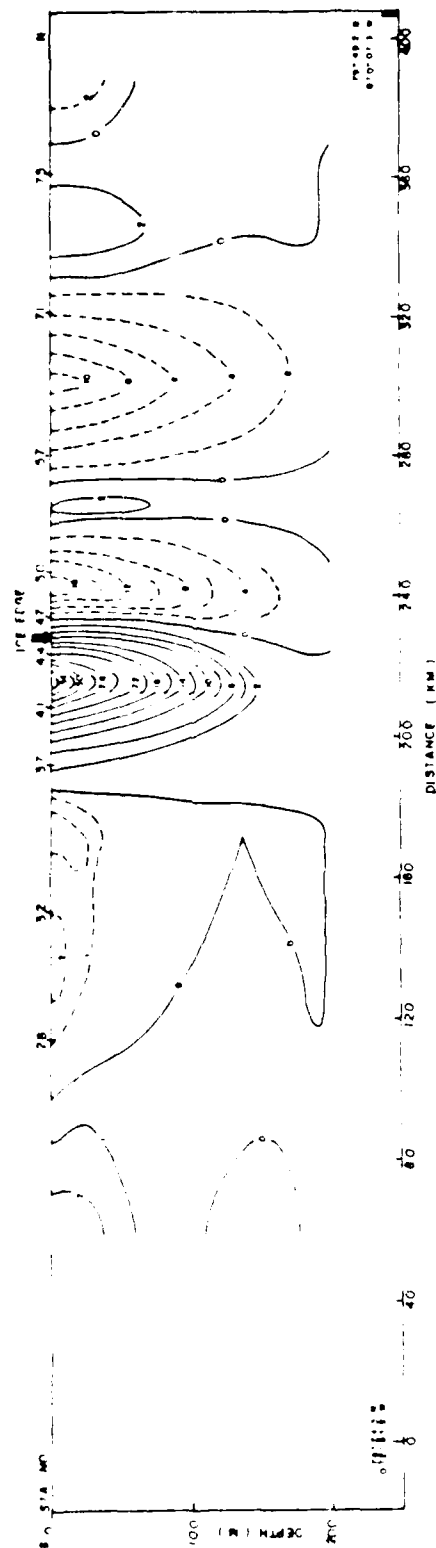
Figure 4.5   A meridional baroclinic velocity cross-section from Baffin Bay northward to Kane Basin. Positive isotachs indicate flow to the west.
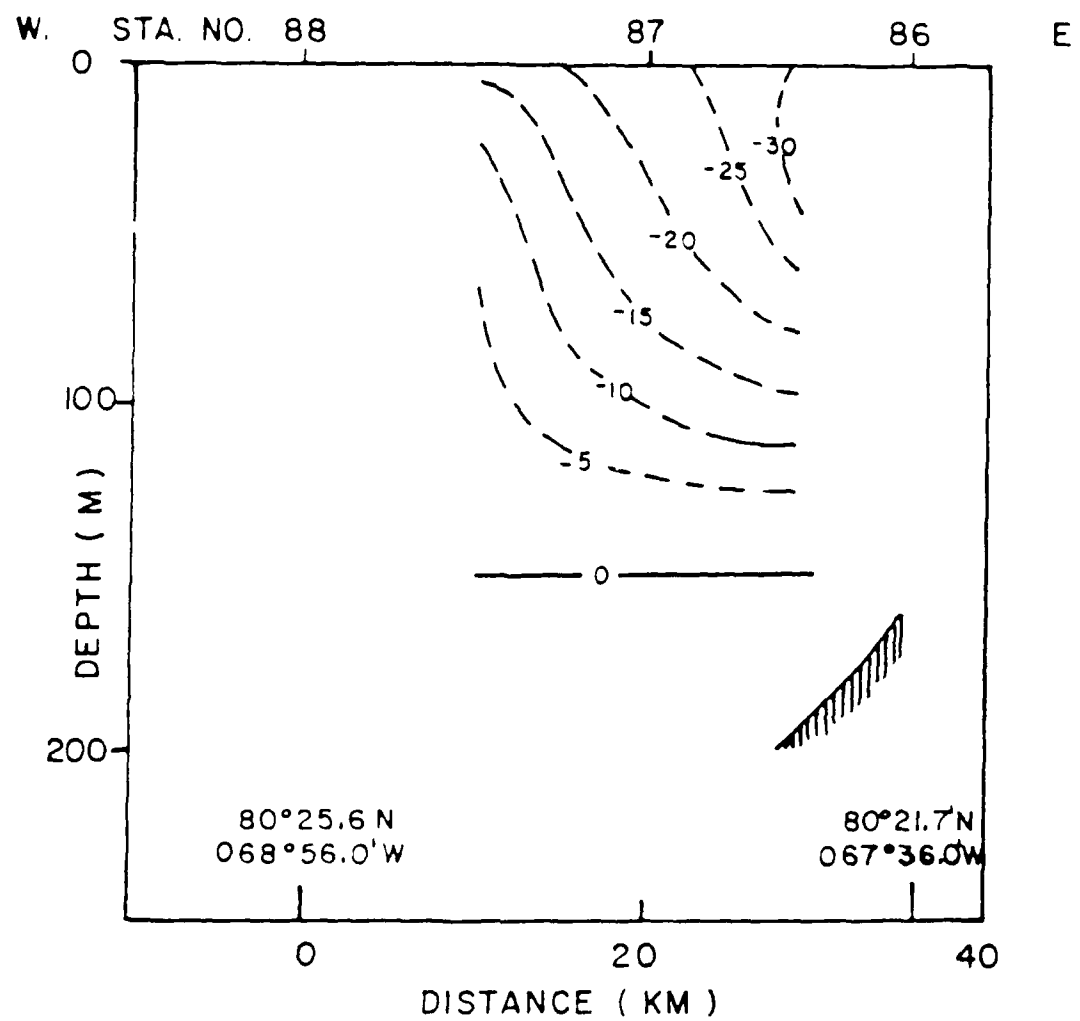
Figure 4 6   A baroclinic velocity cross section through a
southern part of Kennedy Channel.

Figure 3.19), it is probable that the relatively high current speeds in
this area are associated with constriction of flow. Furthermore,
shoaling is more extreme on the eastern side of the channel resulting in
correspondingly higher speeds. In contrast, the high baroclinic current
speed in Robeson Channel is probably due to the influence of the
previously described local concentration of meltwater.

Circulation in Kane Basin is characterized by southward flow in two
peripheral branches surrounding a central cyclonic gyre. Circulation
along the eastern side of Kane Basin is topographically steered
southward along the inherently shallow seabed. Augmented by runoff from
the Humboldt Glacier, this eastern branch continues southwestward and
merges with recurved WGC water in Smith Sound. The flow of the western
branch is also bathymetrically influenced. A portion of this branch
turns cyclonically along the 200 m isobath forming a gyre, while the
remainder continues southward, merging with both the western branch and
the recurved WGC. The southern portion of the gyre is quite apparent in
a baroclinic velocity cross section through Kane Basin (Figure 4.7).

In contrast to its effect on the WGC, topographic steering does not
appear to play as strong a role in Kane Basin. This implies that
circulation within Kane Basin has a significant baroclinic component of
flow. This presumption is most apparent between Stations 74 and 76, at
the northern edge of the gyre. Baroclinic velocities between these
stations reverse from southward at the surface, to northward below 60 m
depth. This vertical shear in velocities is indicative of baroclinic
instability, which might serve as a potential energy source for either
the Kane Basin Gyre or smaller mesoscale features.
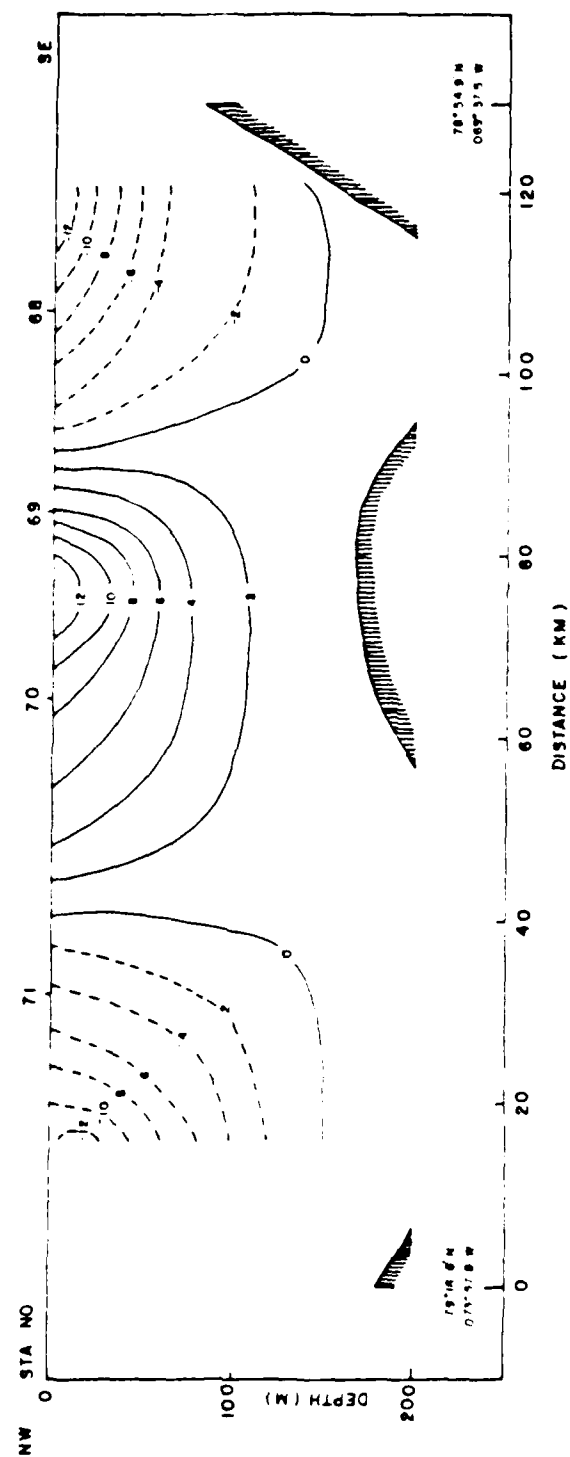
Figure 4.7   A baroclinic velocity cross section through the southern portion of the Kane Basin Gyre.

69

E. THE BAFFIN CURRENT

The Baffin Current originates in Smith Sound, where southwestward flow from Nares Strait merges with recurved WGC water. During its progression southward, the Baffin Current is augmented by outflows from Jones and Lancaster Sounds, and by WGC water which has recurved south of Smith Sound.

As a typical western boundary current, the Baffin Current can be considered highly baroclinic. A baroclinic velocity profile between Stations 28 and 29, assuming a level of no motion at 400 m, indicates surface flow of 0.19 m/sec steadily decreasing to 0.5 m/sec at 200 m. Unlike the WGC, significant baroclinicity in the Baffin Current is not confined to the upper 100 m.

Interaction between the Coriolis force and bathymetry provides the primary steering influence for the Baffin Current. Throughout the course of the current, the tendency for westward turning by the Coriolis force is offset by the presence of a lateral boundary. At the northern entrance to Jones and Lancaster Sounds, however, the removal of this restriction permits the observed westward intrusion of flow. It should be emphasized, however, that the barotropic component of flow associated with the Baffin current is not negligible. An examination of the baroclinic velocity cross section from Jones Sound eastward to Thule provides three clear cases of topographic steering (in conjunction with Figure 4.4, refer to Figure 4.1). Although a branch of the Baffin Current turns westward into Jones Sound, the main core of the current proceeds southward between Stations 2 and 3.

bathymetry. Also apparent are two cyclonic gyres; one around Coburg Island, and the other in the vicinity of a 150 m bank.

Eastward outflow from the south side of Jones Sound subsequently merges with the main core of the Baffin Current along the coast of Devon Island. In contrast to the narrow filament entering Jones Sound, the major branch of the Baffin Current forms the westward intrusion of flow into Lancaster Sound.

F. CIRCULATION IN THE SOUNDS

1. Introduction

Smith, Jones and Lancaster Sounds are all considered regions of net volume inflow to northern Baffin Bay. An examination of the circulation characteristics associated with each sound will provide a basis for their comparison.

2. Smith Sound

Within Smith Sound exists a frontal boundary separating southward flowing ABPW and recurved WGC water. Circulation in this region, therefore, is determined primarily by baroclinic influences. A baroclinic velocity cross section through Smith Sound reveals a weak core between Stations 41 and 4? which is actually the remaining branch of the northward flowing WGC (Figure 4.8). Complete recurvature of this branch occurs just north of Station 41. Southward flow between Stations 42 and 43 is a filament of ABPW from the east branch of circulation in Kane Basin. The interaction between recurved BBSW and southwestward flowing ABPW is marked by the presence of a distinct ice edge. Indeed, the impingement of warm BBSW on the ice edge creates a meltwater gradient which locally elevates the dynamic heights, providing a strong

71
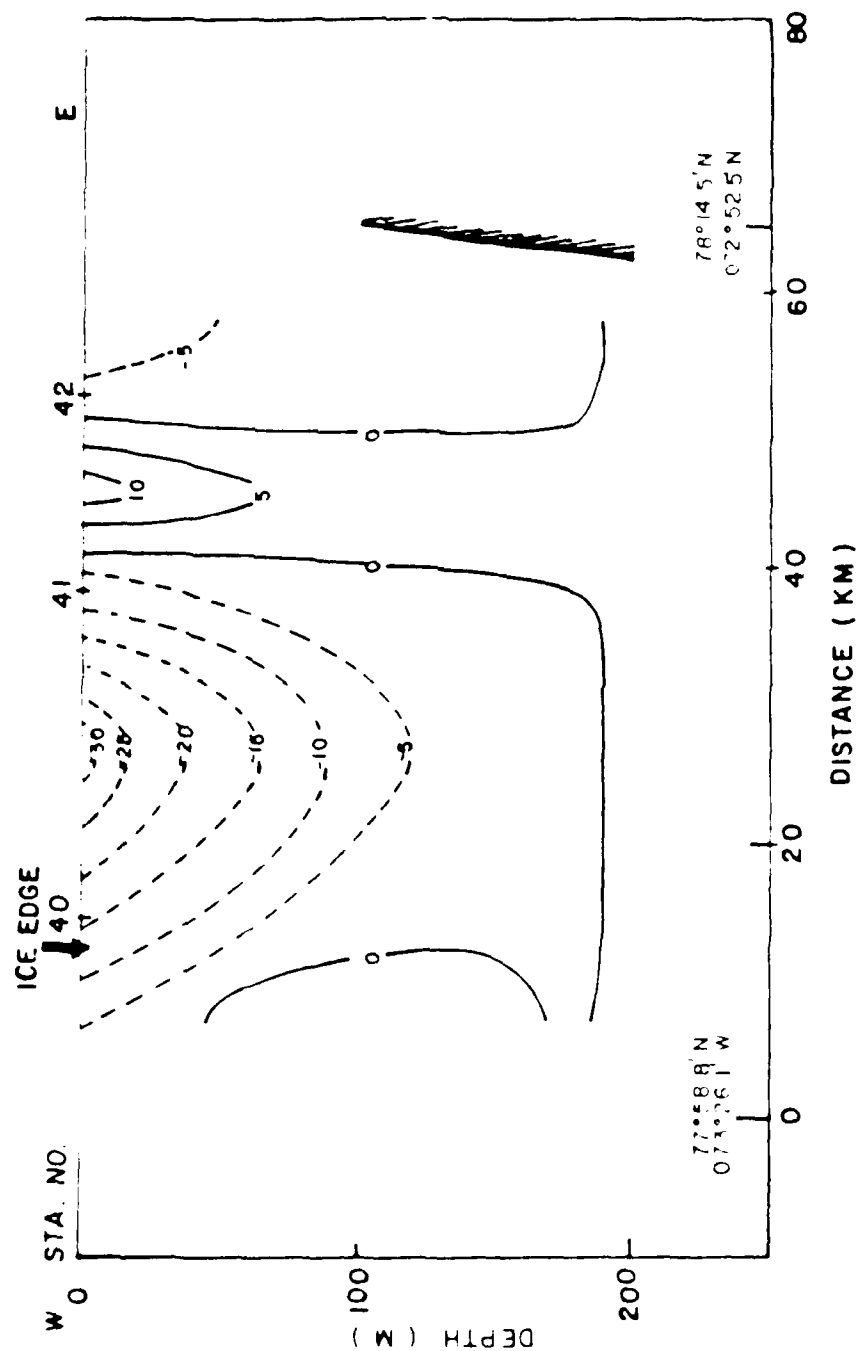
Figure 4.8   A baroclinic velocity cross section through Smith Sound.

baroclinic influence on flow direction. The resultant formation of an
ice edge jet between Stations 40 and 41 marks the origin of the Baffin
Current. Augmentation of the Baffin Current by ABPW occurs beneath the
shallow pycnocline, which is associated with relatively warm, buoyant
BBSW from the WGC (refer to Figure 3.4).

Significant bathymetric influence in Smith Sound is limited to
positioning of the frontal boundary between the two circulation regimes.
Although topographic steering along the 500 m isobath clearly influences
re urvature of the WGC, baroclinic effects are responsible for the
formation of the Baffin Current. Smith Sound, therefore, is the site
where a significantly barotropic circulation regime is transformed into
a predominantly baroclinic one.

3. Jones Sound

The combined influence of bathymetry and the Coriolis force on
the circulation structure of Jones Sound is most apparent in a cross
section of baroclinic velocities (Figure 4.9). A filament of the Baffin
Current is deflected westward by the Coriolis force around the
southeast corner of Ellesmere Island and into Jones Sound north of
Station 15. Eastward outflow of ABPW is restricted to the south of
Station 15, continuing along the east coast of Devon Island. The
presence of a cyclonic gyre around Coburg Island (refer to Figure 4.1)
links the flow paths accordingly.

While eastward outflow from Jones Sound tends to follow the
500 m isobath, the westward intrusion is driven by the Coriolis force
over a 200 m bank, against prevailing westerly winds. The baroclinic
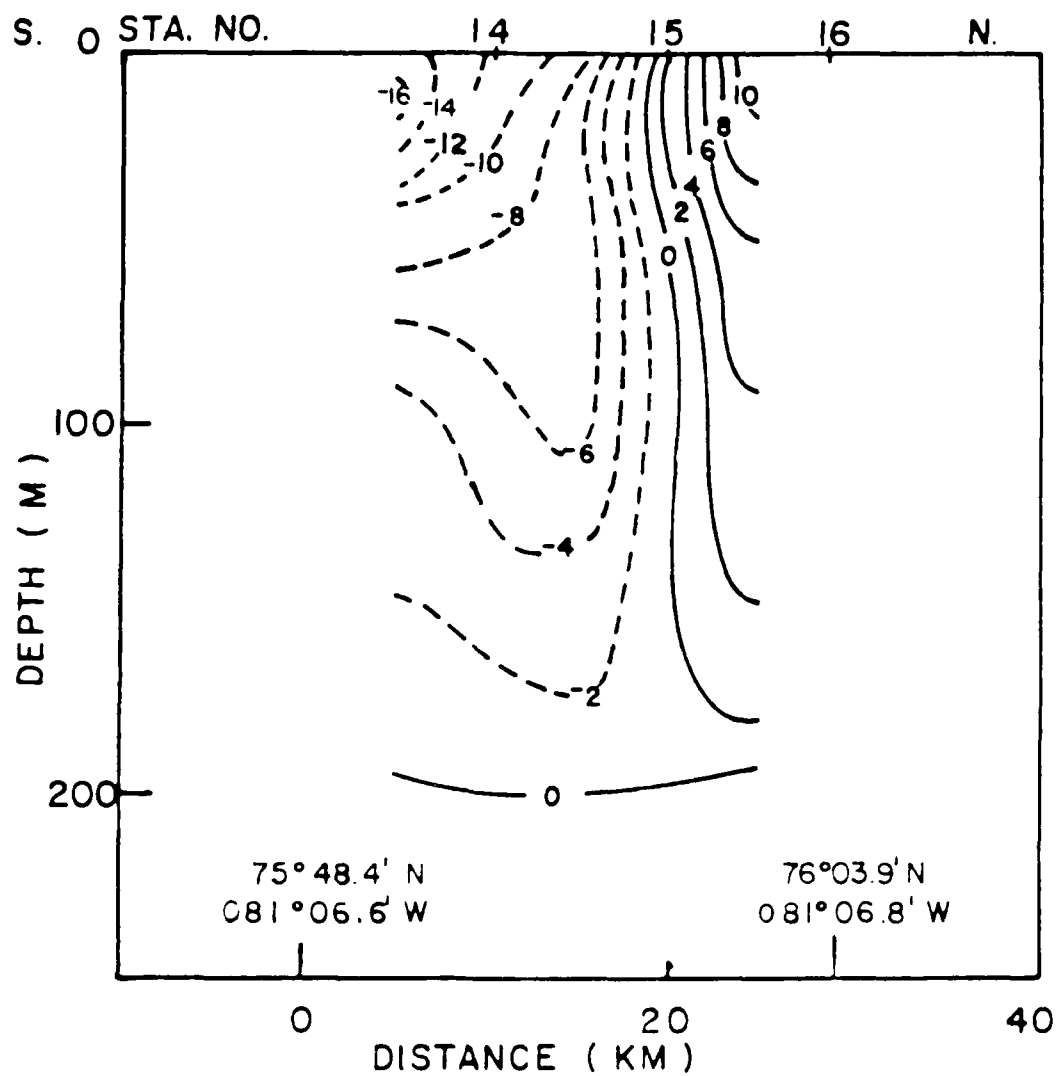
Figure 4.9   A baroclinic velocity cross section through Jones Sound

74

velocity cross section illustrates the relatively shallow nature of this westward intrusion of flow.

4. Lancaster Sound

Circulation in Lancaster Sound is characterized by a westward intrusion of flow between Stations 6 and 9, and an eastward return current of greater magnitude between Stations 1 and 6 (Figure 4.10) The increase in velocities towards the sides of the sound indicates the effect of the Coriolis force on the inflow and outflow branches. Baroclinic velocities in the outflow branch are the highest in the entire NBB-NS region, reaching a maximum of 0.78 m/sec at the surface between Stations 2 and 3 (assuming a level of no motion at 340 m).

5. Geostrophic Estuarine Circulation

Although their thermohaline and bathymetric features are inherently different, the general characteristics of circulation in Smith, Jones and Lancaster Sounds are remarkably similar. In each case, geostrophically balanced inflow is entrained, in estuarine fashion, by geostrophically balanced outflow. A quasi-vertical frontal feature initially separates the two current regimes, the slope of which is determined by their respective velocity structures (refer, for example, to Figure 4.10). The dynamic aspects of the ensuing model, hereinafter referred to as Geostrophic Estuarine Circulation (GEC), are derived from the work of Leblond (1980). Variations in the observed character of the circulation in each sound can be explained in terms of how closely local conditions approximate GEC.

In proposing a two layer "Coastal Current Model" to explain the observed circulation in some channels of the Canadian archipelago,

75
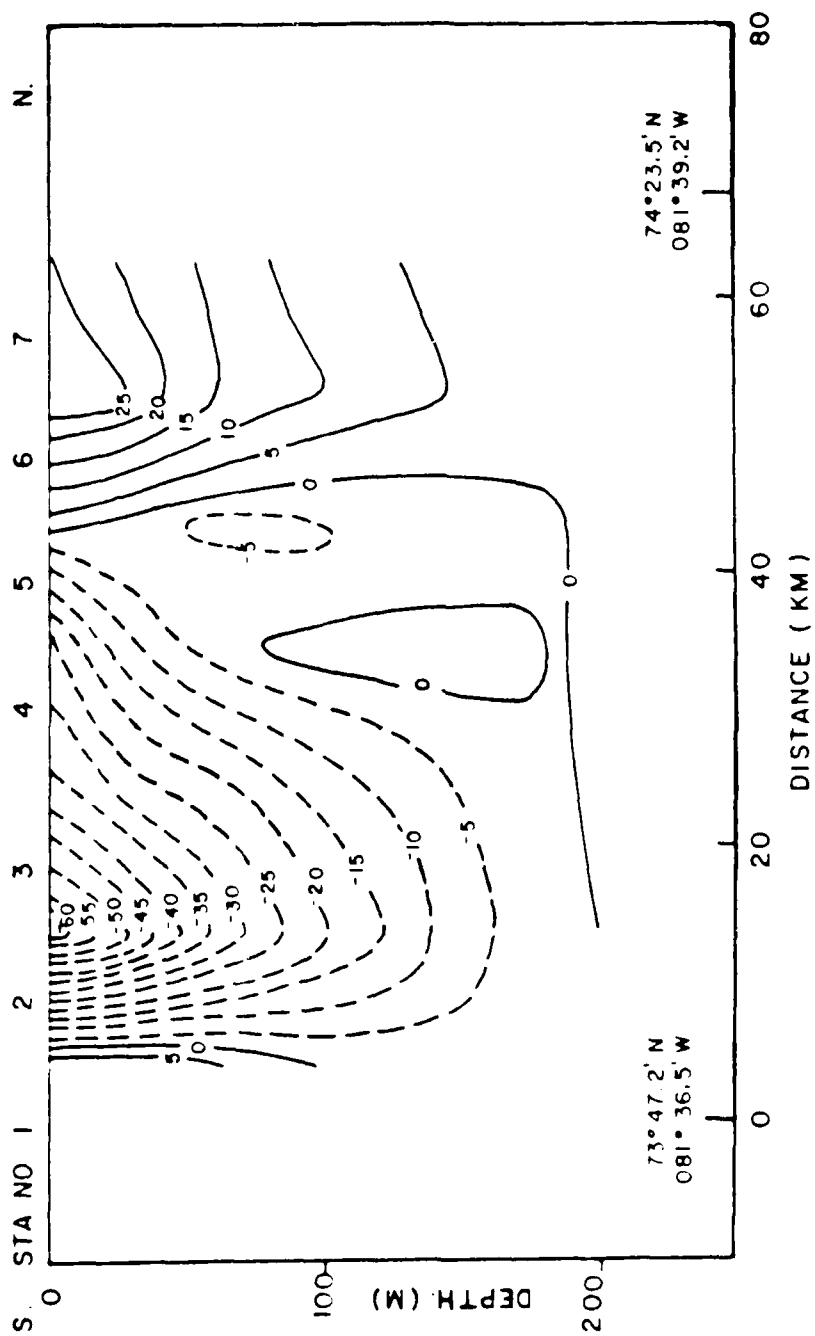
Figure 4.10 A baroclinic velocity cross section through Lancaster Sound

76

Leblond showed that two geostrophically balanced, upper-layer flows would coexist without interference in a channel whose width is sufficiently large compared to the local internal Rossby radius of deformation. Restriction of flow to the upper layer creates a sloped interfacial surface, resulting in a characteristically wedge-shaped velocity structure (Figure 4.11)
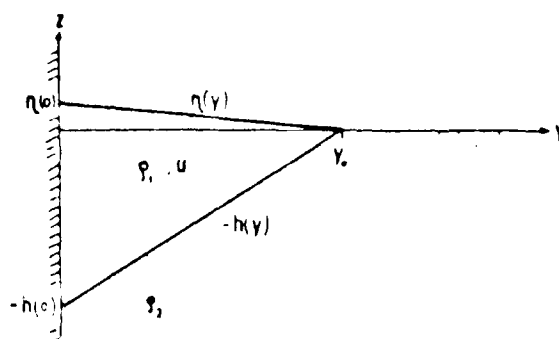
Figure 4.11   A schematic cross section of coastal upper layer flow (out of the page) of speed u, driven by a sea surface slope $\eta(\cdot)$ The lower layer of density ρ_2 is at rest because the interface h(v) slopes in a direction opposite to that of the free surface. Y_0 is the distance from the coast at which the thickness of the upper layer vanishes (from Leblond, 1980, p. 191).

Additionally, Leblond found that purely geostrophic flow can turn corners without separating from a coast if the radius of curvature of the coast is large enough that the Rossby number remains well below unity. As a conservative estimate of the width of a coastal geostrophic current, Y_0 is defined as $Y_0 = R/F$; where R is the internal Rossby radius of deformation and F is the internal Froude number. If the width of a channel is shown to exceed 2 (Y_0), two geostrophically balanced upper-layer flows can theoretically exist without interference

The results of applying Blond's equations to Smith, Jones and Lancaster Sounds are listed in Table II, with the requisite calculations presented in the Appendix. Since the computed Rossby number (R_O) at the mouths of all three sounds is less than 0.1, nonlinear effects may be locally neglected. It should be noted that values of Y_O are only calculated for the outflow regimes which, in each sound, were the widest of the two currents.

Conditions in Lancaster Sound, with a minimum channel width (L) of 80 km, and a geostrophic current width (Y_O) of 20.35 km, most closely approximate GEC. Referring to the baroclinic velocity cross section through Lancaster Sound (Figure 4.10), it clear that although the calculated value of Y_O is considered an underestimation of the width of the outflow current, interference between the two circulation regimes appears negligible. The obvious wedge-shaped current structure implies that flow is primarily restricted to the upper 150 m. The broadening of the outflow wedge beyond the calculated value of Y_O, however, indicates that this restriction is not complete. Indeed, the likelihood of significant flow occurring below 250 m depth is confirmed by the presence of WGAIW in western Lancaster Sound.

Entrainment of inflow results in cyclonic cross-channel flow. The connection of inflow and outflow currents in Lancaster Sound by cross-channel flow was most recently investigated by Fissel et al (1982), who found the westward extent of the inflow intrusion strongly marked by dynamic height anomalies (Figure 4.11). This result illustrates that, in GEC conditions, cross-channel flow is associated with entrainment of inflow by outflow currents. However, the

TABLE II GEOSTROPHIC ESTUARINE CIRCULATION MODEL CALCULATIONS

	Rossby Number (R_0)	Densimetric Froude Number (F)	Internal Rossby Radius	Geostrophic Current Width (Y_0)	Minimum Channel Width (L)
Lancaster Sound	0.06	0.42	8.5 km	20.4 km	80 km
Smith Sound	0.07	0.24	7.3 km	30.3 km	60 km
Jones Sound	0.02	0.21	5.4 km	25.3 km	35 km
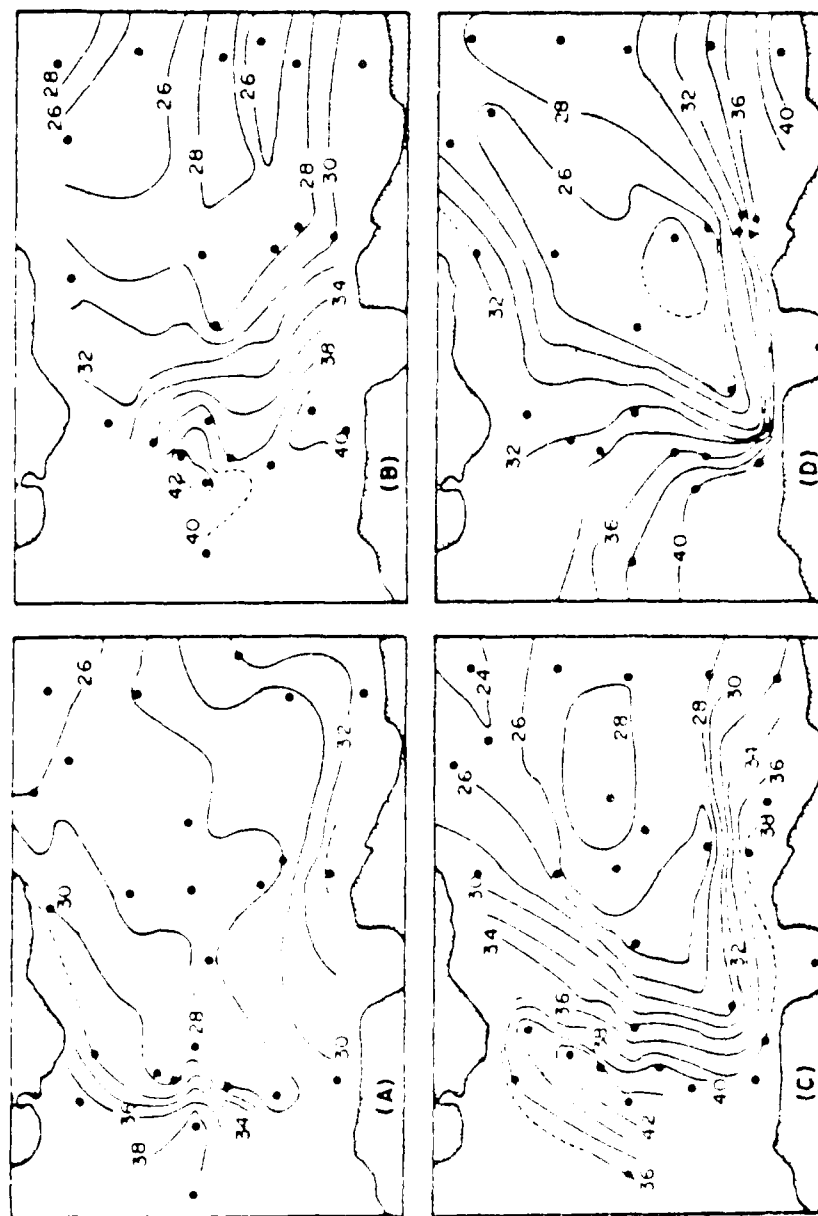
Figure 3.13 Surface dynamic height anomalies in eastern Lancaster Sound (in dynamic cm) relative to the 300 dbar level for four periods of CTD observations in 1979. (A) July 18-19, (B) July 29 - August 3; (C) September 3-6, and (D) September 14-23 (from Fissel et al., 1982, p. 185).

84

convergence of inflow and outflow regimes creates a local elevation in the sea surface, generating geostrophic flow normal to the resultant pressure gradient. With sufficient eastward outflow and the presence of lateral boundaries, characteristic cyclonic flow will result. Since convergence implies downwelling, a reduction in vertical density gradients may occur along this frontal feature, thereby enhancing the tendency for mixing.

In Lancaster Sound the eastward outflow branch of the circulation illustrates the increase in volume and velocity typically associated with estuarine entrainment. In GEC, however, the entrainment is geostrophically, not turbulently, driven.

The application of GEC to Smith Sound is influenced by both geometric constraints and significant horizontal density gradients. Referring to Table II, it is apparent that L is approximately equal to $2 (Y_0)$. Since this is considered a minimum requirement, the potential for interference between the inflow and outflow regimes may be significant. This interference may manifest itself in the form of baroclinic instability and associated eddy generation.

Within Smith Sound the inflow and outflow regimes are not appreciably influenced by coastal boundaries. The absence of a characteristically wedge-shaped velocity structure in this region is probably a consequence of this fact. Geostrophy does influence the direction of the inflow and outflow branches, however, resulting in cyclonic cross-channel flow. As stated previously, recurvature of the remaining branch of the WGC occurs as the result of an extreme horizontal density gradient at the inside front. Entrainment of WGC

81

inflow in Smith Sound, while not directly attributed to convergence, is nonetheless geostrophically balanced.

The limitations in applying GEC to Jones Sound are considerable. Since $L < 2(Y_0)$, Jones Sound is wide enough to accommodate only one geostrophically-balanced current. Referring to the 33.0 isohaline in Figure 3.14, the formation of density and, hence, baroclinic velocity wedges is evident at the sides of the channel; however, a complete blurring of the structure occurs between Stations 14 and 15. Since these current branches can not coexist in Jones Sound, it may be possible for complete intrusion of the westward inflow branch to occur at times, resulting in reversal of the net eastward flow in Jones Sound. Historical evidence of this occurrence has been cited by Muench (1971) (Figure 4.13). In 1962, for example, the flow is entirely westward, while in 1963 both inflow and outflow are present simultaneously but with the outflow dominant.

The macroscale circulation pattern in the NEB-NS region can also be envisioned as conforming to the GEC model. Viewed simplistically, the inflowing waters of the WGC are geostrophically entrained at various latitudes, subsequently resulting in the augmented outflow which characterizes the Baffin Current. The predictably cyclonic circulation pattern associated with GEC is identifiable as a major macroscale feature in the region.

G. BAROCLINIC TRANSPORTS

Baroclinic transports derived from various arbitrary reference levels should be used only with the intention of interpolating of volume. This is especially true in eastern boundary current regions.

82
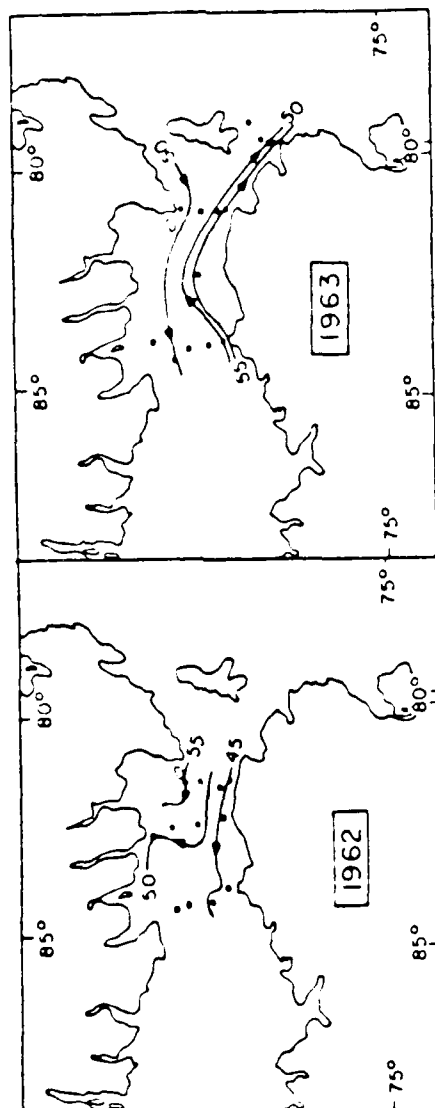
Figure 4.13 Dynamic topography of the surface relative to 500 dbars in Jones Sound for various years; (from Muench, 1971, p. 92).

83

like the WGC, where the baroclinicity is known to be weak. The main
purpose of this section, therefore, will be to qualitatively compare the
baroclinic components of flow for major currents in the NBB-NS region
Unless otherwise specified, subsequent references to transports are
summarized in plan view and assumed to be baroclinic in nature
(Figure 4.14).

The WGC achieves maximum transport in Melville Bay, prior to its
previously described pattern of recurvature in northern Baffin Bay and
Smith Sound. Transport of the WGC consequently decreases from a
maximum of 0.7 Sv in Melville Bay, to 0.4 Sv in the vicinity of the
Carey Islands, and 0.2 Sv in Smith Sound. The major portion of
baroclinic transport is concentrated at the extreme inshore stations in
Melville Bay, further substantiating the assumption that glacial runoff
is primarily responsible for this component of WGC flow.

The Baffin Current is partially derived from the net southward flow
of Nares Strait. Southward transport increases from 0.2 Sv in Robeson
Channel to 0.7 Sv at the mouth of Kennedy Channel. This increase may be
attributed to admixture of meltwater runoff, in particular from
Petermann's Glacier, located on the eastern shore of Robeson Channel.
Southward transport through Kane Basin is primarily associated with the
western circulation branch (0.3 Sv), while southward transport in the
eastern circulation branch is limited (0.1 Sv). The swirl transport
within the Kane Basin Gyre is approximately 0.4 Sv, indicative of its
effect in recirculating meltwater from the Humboldt Glacier throughout
the basin. The cyclonic ice-edge jet in Smith Sound, with associated
transport of 0.5 Sv, can be considered as the outflow from Nares Strait
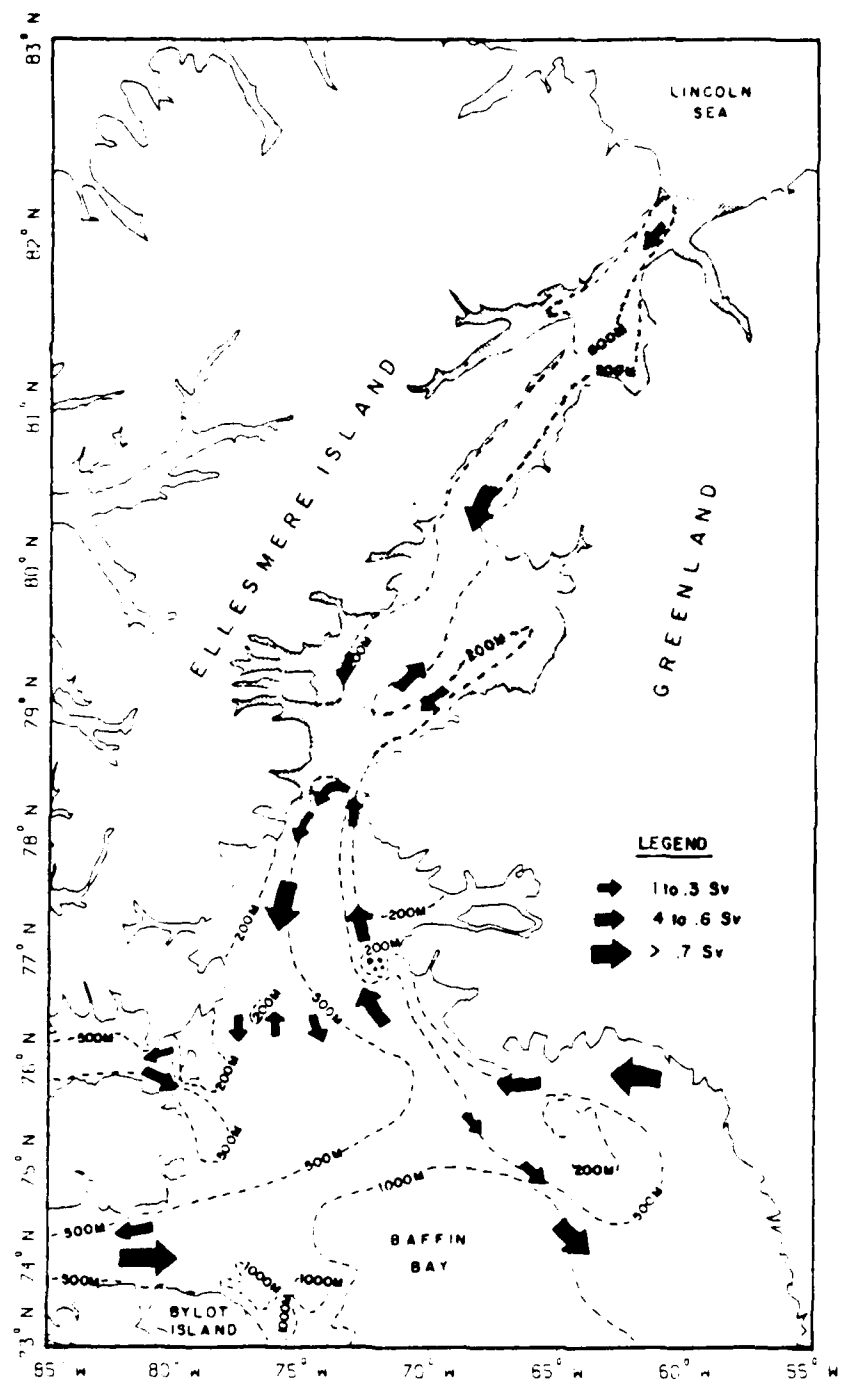
Figure 4.14   Major baroclinic transports in the NBB-NS
region.

85

which is augmented by entrainme t of the remainder of the sou to 2 Sv.
Net southward outflow from Kane Basin through Smith Sound, therefore, is
inferred to be approximately 0.4 Sv.

The Baffin Current, which becomes an identifiable feature in Smith
Sound, continues southward along the coast of Ellesmere Island where
transport is measured as 1.0 Sv. The formation of a topographically
induced cyclonic gyre is coincident with branching of the Baffin
Current northeast of Coburg Island. A westward flowing filament (0.1 Sv)
enters Jones Sound, where it is entrained and augmented by eastward
outflow (0.4 Sv), resulting in net eastward transport of 0.3 Sv. A
southwestward flowing branch (.2 Sv) probably follows the 500 m
isobath, subsequently merging with the main core of the Baffin Current.
The relatively large transport (0.7 Sv) indicated southwest of Melville
Bay is actually an algebraic summation of transports obtained between
Stations 127 and 132 (refer to Figure 4.3). Southeastward transport of
Baffin Current water (0.4 Sv), probably derived from a bra h of
Lancaster Sound outflow which is topographically steered eastward along
the 1000 m isobath (Muench 1971), is apparent southwest of Station 130.
Flow of WGC water, which has recurved either around the shallow bank in
Melville Bay (0.2 Sv) or south of the Carey Islands (0.1 Sv), is
indicated between Stations 127 and 129.

The main core of the Baffin Current, augmented by eastward outflow
from Jones Sound, follows the southwest coast of Devon Island westward
into Lancaster Sound (0.6 Sv). GEC entrainment and subsequent
augmentation of outflow yields gross east und outflow of 1.7 Sv. Net

transport in Lancaster Sound, therefore, is inferred to be 1.1 Sv
eastward.

V.   THE NORTH WATER PROCESS

The North Water Process is characterized by complex interaction between thermohaline and dynamic effects. The net result of this process is the demarcation of an 80,000 km^2 arctic region which is conspicuously devoid of first year ice from the onset of winter until March (Steffen and Ohmura 1985). Following a brief examination of some relevant factors, a qualitative description of the process will be presented.

In southern Baffin Bay freezing is generally accompanied by the formation of an isothermal isohaline near-surface layer approximately 75 m to 100 m in depth (Garrison et al., 1976). Sea-ice production in the NBB-NS region is similarly associated with the formation of such deep mixed layers (Muench, 1971). In the weakly stratified waters of Nares Strait, convective processes are sufficient to form this homogenous layer. The region south of Smith Sound, however, is characterized by the ubiquitous occurrence of BBSW. The resultant presence of such a strong pycnocline would ordinarily limit the depth of convective mixing associated with surface freezing to much less than 75 m. A combination of turbulent and convective processes must be required, therefore, to overcome the inherent stability of this buoyant layer and produce the observed deep mixed layers.

Given a particular set of climatic conditions, the enthalpy present in the near-surface layer determines the length of time required to initiate surface freezing. Assuming heat flux only through the surface and neglecting thermal advection, it is possible to evaluate this time delay as a function of heat budget parameters   Steffen and Ohmura

88

(1985) computed monthly and annual heat budgets for the North Water
region and concluded, assuming a reference temperature of -1.8°C, that
the amount of oceanic heat flux required to prevent ice formation is
337.4 MJM^{-2} in October and 445.1 MJM^{-2} in November. The enthalpy
contained in the 75-m deep, near-surface layer was calculated,
referenced to -1.8°C, for all FRANKLIN 86 stations (Figure 5.1). For 22
stations located southward of Smith Sound, between 76° N and 78° N, the
enthalpy in September averaged 475 MJ. Applying the aforementioned heat
budget at the onset of winter (October), implies that surface freezing
would be delayed by approximately five weeks in this region. In
contrast, the average enthalpy contained in the ice-covered, near-
surface layer north of 78°N (Nares Strait) was 120 MJ.

The presence of mechanical ice removal effects such as divergent
currents and winds will cause the rate of sea-ice production to greatly
exceed the rate of sea ice accumulation for a given area. This
phenomena is graphically illustrated in the vicinity of the Kane Basin
Gyre where cyclonic and, hence, divergent circulation results in an area
of reduced ice concentration. Ice concentrations within the gyre were
typically 3/10 or less, compared with surrounding concentrations of
greater than 5/10. The cyclonic macroscale circulation pattern
characteristic of northern Baffin Bay can be expected to provide a
similar mitigating influence on the accumulation of sea-ice. The
potential influence of persistent northerly winds on the reduction of
sea-ice concentration in northern Baffin Bay has been discussed by
Muench (1971) and Dunbar (1973).
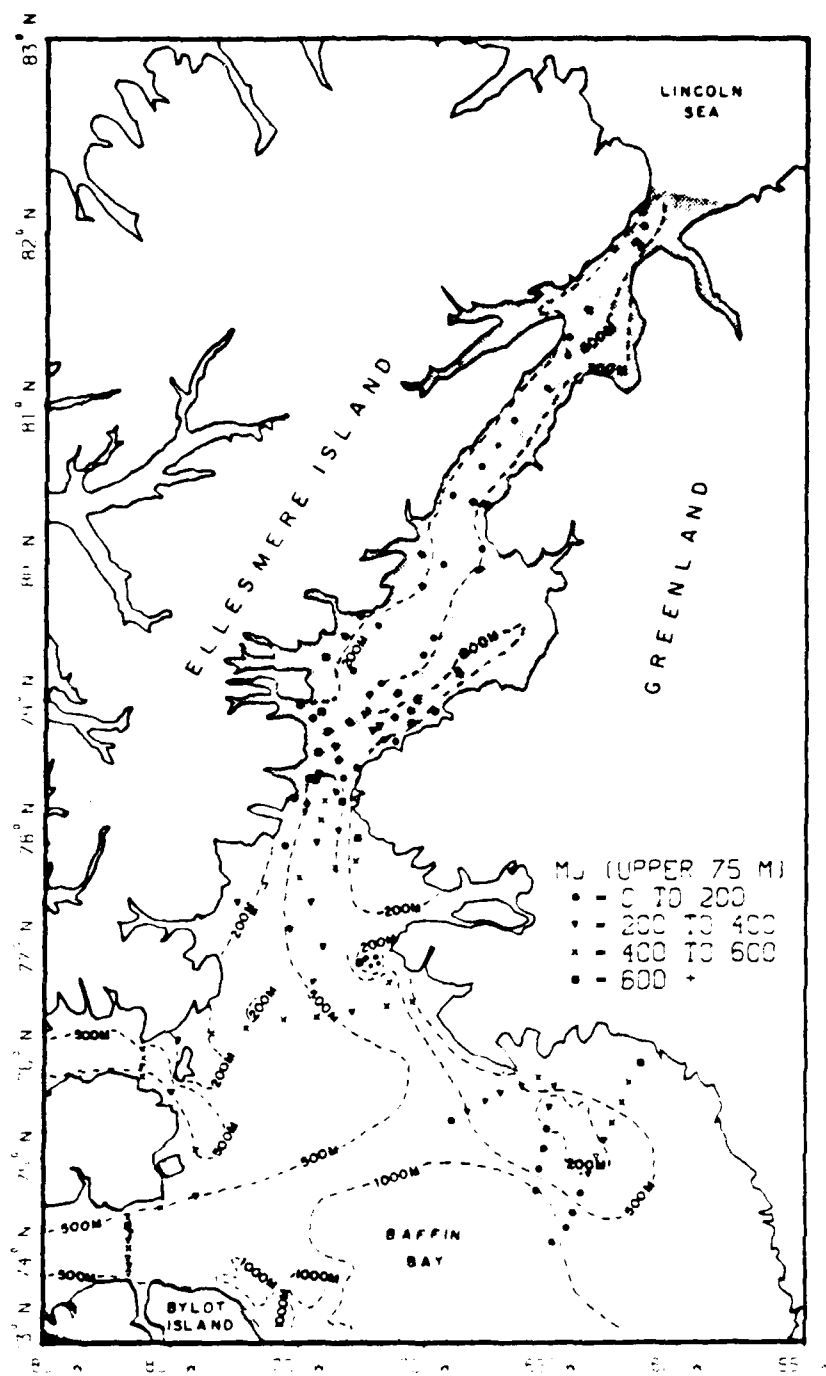
Figure 5.1   Enthalpy of the near surface (upper 75 m)
               layer in the NBB-NS region (referenced to
               - 1.8°C).

90

The North Water Process results from the combined influences of near-surface layer enthalpy and mechanical ice removal. Since the North Water is characterized by reduced ice coverage, the associated decrease in albedo results in the largest annual net radiation for any region within the Arctic Circle (Steffen and Ohmura, 1985). Admixture of glacial runoff creates a strong, shallow pycnocline which effectively confines insolation effects to the near-surface layer. Such inherent stratification would normally restrict convective overturn associated with surface freezing to shallower depths. Mechanical ice removal, however, results in a proportionally greater rate of brine formation which increases the vertical extent of mixing. Complete removal of the enthalpy in this near surface layer delays significant sea-ice formation accordingly. Divergent cyclonic currents and northerly winds then serve to reduce sea-ice accumulation for the remainder of winter. It is the self-perpetuating nature of the North Water Process which accounts for its persistence.

VI. DISCUSSION

The comprehensive nature of this analysis mandates further examination of certain relevant topics. A combination of elaboration and postulation will be employed in this regard.

The dilution of WGC water masses, relative to those which enter the NBB-NS region through the Canadian Archipelago, is a consequence of the more extensive shelf-driven modification effects inherent in the former. The assertion by Muench (1971), that the major proportion of Arctic Ocean Water is less dense than Baffin Bay Water, was derived from point data sources, under the assumption that there are significant differences in water structures between the upper 250 m layers of the Arctic Ocean and Baffin Bay. Muench further concludes that these water-structure differences create a proportionally higher surface elevation in the Arctic Ocean, resulting in net southward transport.

An examination of the dynamic topography of the NBB-NS region reveals an obvious lack of north-south dynamic height gradients (refer to Figure 4.2). This is due to the fact that ABPW and WGCPW have a common origin in the Arctic Basin, and are quite similar in thermohaline character. What is apparent, however, is a distinct dynamic height gradient normal to the coastline. Although the increase in dynamic heights in the onshore direction can be viewed as a consequence of the influence of the Coriolis force on the prevailing baroclinic flow, it may alternately be considered as a driving force for the observed circulation in the NBB-NS region.

The ubiquitous glaciers in the region provide a significant coastal source of meltwater, an influence that may be expected to drive a

geostrophically-balanced current with the shoreline on the right, in the direction of flow. The implication of this hypothesis is that a progressive winter weakening in near-surface currents would be expected throughout the NBB-NS region. Lemon and Fissel (1982) provided evidence of just such an occurrence in northwestern Baffin Bay.

On a larger scale, the concentration of glacial meltwater within the NBB-NS region results in near-surface layer dilution relative to the saltier waters of the North Atlantic. It is the difference in near-surface water structure between these regions that may drive the net southward baroclinic transport. A progressive winter decrease in this net southward transport would be expected accordingly.

VII. CONCLUSIONS

The physical oceanography of the northern Baffin Bay - Nares Strait region has been investigated using a dense network of CTD stations occupied by the CCGS SIR JOHN FRANKLIN in September 1986. The following major conclusions can be drawn:

* Five water masses can be delineated in the region. The WGC is the source of WGCPW and WGCAIW, while ABPW and NSAIW are derived from the Arctic Basin via the Canadian Archipelago. WGCAIW and NSAIW are prevented by shoaling of the sea floor from entering Smith Sound and Kane Basin, respectively. BBSW is found seasonally throughout northern Baffin Bay.

* The waters unique to the WGC are subject to more extensive dilution effects by shelf-driven processes and are comparatively less saline than their Canadian Archipelago derived counterparts.

* Bathymetry provides a significant influence on the flow of the WGC, which attains a maximum baroclinic transport of 0.7 Sv in Melville Bay. Recurvature of component branches of the WGC occurs primarily in Melville Bay (0.2 Sv), south of the Carey Islands (0.1 Sv), and ultimately in Smith Sound (0.2 Sv).

* The Baffin Current originates as an ice edge jet in Smith Sound subsequently proceeding southward along the coast of Ellesmere Island and throughout northern Baffin Bay and its upper portions
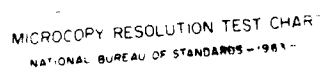
MICROCOPY RESOLUTION TEST CHART

NATIONAL BUREAU OF STANDARDS - 1963

Baffin Current is augmented by net outflow from Kane Basin, Jones Sound and Lancaster Sound at rates of 0.3 Sv, 0.3 Sv and 1.1 Sv, respectively.

* Circulation in Smith, Jones and Lancaster Sounds can be described in terms of the GEC model, in which estuarine inflow, entrainment and outflow are geostrophically balanced processes.

* Although a significant portion of the meltwater derived from the Humboldt Glacier is recirculated by the Kane Basin Gyre (0.4 Sv), the influence of glacial admixture on thermohaline structure and near-surface circulation is apparent throughout the NBB-NS region.

* The North Water Process results from the combined influences of near-surface layer enthalpy and mechanical ice removal.

<u>APPENDIX</u>

COMPUTATIONS ASSOCIATED WITH THE GEC MODEL

The computation of geostrophic current widths in Smith, Jones and Lancaster Sounds is accomplished as prescribed by Leblond (1980). The requisite equations and calculations are presented here.

The "Coastal Current Model" of Leblond (1980) assumes geostrophic flow confined to the upper layer of a two-layer stratified fluid, in a channel of width L and depth H (refer to Figure 4.11). Assuming the upper layer is relatively thin with respect to the lower layer, the speed of interfacial waves in the fluid may be approximated as:

$$C^2 = \frac{g(\rho2-\rho_1)\ t(o)}{\rho_1} \tag{1}$$

where: g — the gravitational acceleration;

ρ_1 — the density of the upper layer;

ρ_2 — the density of the lower layer; and

$t(o)$ — the thickness of the upper layer at the channel wall.

In Smith Sound: $\rho_1 = 1025.5$ kg/m^3; $\rho_2 = 1027.0$ kg/m^3; and $t(o)$

$= 75$ m.

In Jones Sound: $\rho_1 = 1026.2$ kg/m^3; $\rho_2 = 1027.0$ kg/m^3; and $t(o)$

$= 75$ m.

In Lancaster Sound: $\rho_1 = 1026.0$ kg/m^3; $\rho_2 = 1027.0$ kg/m^3; and $t(o)$

$= 150$ m.

The internal Rossby radius of deformation is defined as:

$R = C/f$ (2)

where: f — the Coriolis parameter.

The internal Froude number is defined as:

$$F - u/C \qquad (3)$$

where: u — the speed of the upper layer flow.

In Smith Sound: u — 0.25 m/s.

In Jones Sound: u — 0.16 m/s.

In Lancaster Sound: u — 0.50 m/s.

The Rossby number is defined as:

$$R_o - \frac{R}{fr} \qquad (4)$$

where: r — the radius of curvature of the flow.

In Smith Sound: r — 25 km.

In Jones Sound: r — 75 km.

In Lancaster Sound: r — 60 km.

The width of the geostrophic current is then defined as:

$$Y_o - \frac{R}{F} \qquad (5)$$

LIST OF REFERENCES

Aagaard, K., and L.K. Coachman, The East Greenland Current north of the Denmark Strait, I, <u>Arctic</u>, 21, 181-200, 1968.

Bourke, R.H., R.G. Paquette, and A.M. Weigel, MIZLANT 85 data report: results of an oceanographic cruise to the Greenland Sea, September, 1985, Tech. Rep. NPS 68-86-007, Dept. of Oceanography, Naval Postgraduate School, Monterey, California, 1986.

Coachman, L.K. and K. Aagaard, Physical oceanography of Arctic and subarctic seas, in <u>Arctic Geology and Oceanography</u>, edited by Y Herman, pp. 1-72, Springer-Verlag, New York, 1974.

Dunbar, I.M., Winter regime of the North Water, <u>Trans. R. Soc. Can.</u>, 4(9), 275-281, 1973.

Fissel, D.B., D.D. Lemon, and J.R. Birch, Major features of the summer near-surface circulation of western Baffin Bay, 1978 and 1979, <u>Arctic</u>, 35, 180-200, 1982.

Garrison, G.R., H.R. Feldman and P. Becker, Oceanographic measurements in Baffin Bay, Unpublished manuscript, Applied Physics Laboratory University of Washington, February, 1976.

Leblond, P.H., On the surface circulation in some channels of the Canadian Arctic Archipelago, <u>Arctic</u>, 35, 189-197, 1980.

Lemon, D.D. and D.B. Fissel, Seasonal variations in currents and water properties in northwestern Baffin Bay, 1978 and 1979, <u>Arctic</u>, 35, 211-218, 1982.

Melling, H., R.A. Lake, D.R. Topham, and D.B. Fissel, Oceanic thermal structure in the western Canadian Arctic, <u>Continental Shelf Research</u>, 3, 233-258, 1984.

Muench, R.D., The physical oceanography of the northern Baffin Bay region, Baffin Bay-North Water Proj. Arct. Inst. North Am. Sci. Rep., 1-72, 1971.

Muench, R.D., and H.E. Sadler, Physical oceanographic observations in Baffin Bay and Davis Strait, <u>Arctic</u>, 26, 73-76, 1973.

Sadler, H.E., Water, heat, and salt transports through Nares Strait, Ellesmere Island, <u>J. Fish. Res. Board Can.</u>, 33, 2286-2295, 1976.

Steffen, K. and A. Ohmura, Heat exchange and surface conditions in the North Water, northern Baffin Bay, <u>Ann. Glaciology</u>, 6, 178-181, 1985.

Tunnicliffe, M.D., An investigation of the waters of the East Greenland
Current, Master's Thesis, Naval Postgraduate School, Monterey,
California, September 1985.

INITIAL DISTRIBUTION LIST

No. Copies

1. Director
   Applied Physics Laboratory
   Attn: Mr. Robert E. Francois   1
          Mr. E.A. Pence   1
          Mr. G.R. Garrison   1
          Library   1
   University of Washington
   1013 Northeast 40th Street
   Seattle, Washington 98105

2. Director   5
   Arctic Submarine Laboratory
   Code 19, Building 371
   Naval Ocean Systems Center
   San Diego, California 92152

3. Superintendent
   Naval Postgraduate School
   Attn: Dr. R.H. Bourke, Code 68Bf   7
          Dr. R.G. Paquette, Code 68Pa   1
          Dr. D.C. Smith IV, Code 68Si   1
   Monterey, California 93943

4. Polar Research Laboratory, Inc.   1
   6309 Carpinteria Ave.
   Carpinteria, California 93103

5. Chief of Naval Operations
   Department of the Navy
   Attn: NOP-02   1
          NOP-22   1
          NOP-964D2   1
          NOP-095   1
          NOP-098   1
   Washington, District of Columbia 20350

6. Commander   1
   Submarine Squadron THREE
   Fleet Station Post Office
   San Diego, California 92132

7. Commander   1
   Submarine Group FIVE
   Fleet Station Post Office
   San Diego, California 92132

8. Dr. John L. Newton   1
   10211 Rookwood Drive
   San Diego, California 92131

9. Director   1
   Marine Physical Laboratory
   Scripps Institution of Oceanography
   San Diego, California 92132

10. Commanding Officer   1
    Naval Intelligence Support Center
    4301 Suitland Road
    Washington, District of Columbia 20390

11. Commander   1
    Space and Naval Warfare Systems Command
    Department of the Navy
    Washington, District of Columbia 20360

12. Director   1
    Woods Hole Oceanographic Institution
    Woods Hole, Massachusetts 02543

13. Commanding Officer   1
    Naval Coastal Systems Laboratory
    Panama City, Florida 32401

14. Commanding Officer   1
    Naval Submarine School
    Naval Submarine Base, New London
    Groton, Connecticut 06349-5700

15. Assistant Secretary of the Navy   1
    (Research and Development)
    Department of the Navy
    Washington, District of Columbia 20350

16. Director of Defense Research and Engineering   1
    Office of Assistant Director (Ocean Control)
    The Pentagon
    Washington, District of Columbia 20301

17. Commander, Naval Sea Systems Command   1
    Department of the Navy
    Washington, District of Columbia 20362

18. Chief of Naval Research
    Department of the Navy
    Attn: Code 102-OS   1
             Code 220   1
             Code 1125 Arctic   1
    800 N. Quincy Street
    Arlington, Virginia 22217

19. Project Manager   1
    Anti-Submarine Warfare Systems Project
    Office (PM4)
    Department of the Navy
    Washington, District of Columbia 20360

20. Commanding Officer   1
    Naval Underwater Systems Center
    Newport, Rhode Island 02840

21. Commander   1
    Naval Air Systems Command
    Headquarters
    Department of the Navy
    Washington, District of Columbia 20361

22. Commander
    Naval Oceanographic Office
    Attn: Library Code 3330   1
    Washington, District of Columbia 20373

23. Director   1
    Advanced Research Project Agency
    1400 Wilson Boulevard
    Arlington, Virginia 22209

24. Commander SECOND Fleet   1
    Fleet Post Office
    New York, New York 09501

25. Commander THIRD Fleet   1
    Fleet Post Office
    San Francisco, California 96601

26. Commander
    Naval Surface Weapons Center
    White Oak
    Attn: Mr. M.M. Kleinerman   1
           Library   1
    Silver Springs, Maryland 20910

27. Officer-in-Charge   1
    New London Laboratory
    Naval Underwater Systems Center
    New London, Connecticut 06320

28. Commander
    Submarine Development Squadron TWELVE   1
    Naval Submarine Base
    New London
    Groton, Connecticut 06349

29. Commander
    Naval Weapons Center
    Attn: Library   1
    China Lake, California 93555

30. Commander
    Naval Electronics Laboratory Center
    Attn: Library   1
    27, Catalina Boulevard
    San Diego, California 92152

31. Director   1
    Naval Research Laboratory
    Attn: Technical Information Division
    Washington, District of Columbia 20375

32. Director   1
    Ordnance Research Laboratory
    Pennsylvania State University
    State College, Pennsylvania 16801

33. Commander Submarine Force   1
    U.S. Atlantic Fleet
    Norfolk, Virginia 23511

34. Commander Submarine Force
    U.S. Pacific Fleet   1
    Attn: N-21
    Pearl Harbor, Hawaii 96860-6550

35. Commander   1
    Naval Air Development Center
    Warminster, Pennsylvania 18974

36. Commander   1
    Naval Ship Research and Development Center
    Bethesda, Maryland 20084

37. Commandant   1
    U.S. Coast Guard Headquarters
    400 Seventh Street, S.W.
    Washington, District of Columbia 20590

38. Commander   1
    Pacific Area, U.S. Coast Guard
    630 Sansome Street
    San Francisco, California 94126

39. Commander   1
    Atlantic Area, U.S. Coast Guard
    159E, Navy Yard Annex
    Washington, District of Columbia 20590

40. Commanding Officer   1
    U.S. Coast Guard Oceanographic Unit
    Building 159E, Navy Yard Annex
    Washington, District of Columbia 20590

41. Scientific Liaison Office   1
    Office of Naval Research
    Scripps Institute of Oceanography
    La Jolla, California 92037

42. Scripps Institution of Oceanography   1
    Attn: Library
    P.O. Box 2367
    La Jolla, California 92037

43. School of Oceanography
    University of Washington
    Attn: Dr. L.K. Coachman   1
          Dr. S. Martin   1
          Mr. D. Tripp   1
          Library   1
    Seattle, Washington 98195

44. School of Oceanography   1
    Oregon State University
    Attn: Library
    Corvallis, Oregon 97331

45. CRREL
    U.S. Army Corps of Engineers
    Attn: Library   1
    Hanover, New Hampshire 03755-1290

46. Commanding Officer   1
    Fleet Numerical Oceanography Center
    Monterey, California 93943

47. Commanding Officer   1
    Naval Environmental Prediction Research Facility
    Monterey, California 93943

48. Defense Technical Information Center   2
    Cameron Station
    Alexandria, Virginia 22304-6145

49. Commander   1
    Naval Oceanography Command
    NSTL Station
    Bay St. Louis, Mississippi 39529

50. Commanding Officer
    Naval Ocean Research and Development Activity
    Attn: Technical Director   1
    NSTL Station
    Bay St. Louis, Mississippi 39529

51. Commanding Officer   1
    Naval Polar Oceanography Center, Suitland
    Washington, District of Columbia 20373

52. Director   1
    Naval Oceanography Division
    Naval Observatory
    34th and Massachussetts Ave. NW
    Washington, District of Columbia 20390

53. Commanding Officer
    Naval Oceanographic Command   1
    NSTL Station
    Bay St. Louis, Mississippi 39522

54. Scott Polar Research Institute
    University of Cambridge
    Attn: Library   1
           Sea Ice Group   1
    Cambridge, ENGLAND
    CB2 1ER

55. Chairman   2
    Department of Oceanography
    U.S. Naval Academy
    Annapolis, Maryland 21402

56. Dr. James Morison   1
    Polar Science Center
    4057 Roosevelt Way, NE
    Seattle, Washington 98105

57. Dr. Kenneth Hunkins   1
    Lamont-Doherty Geological Observatory
    Palisades, New York 10964

58. Dr. David Paskowsky, Chief   1
    Oceanography Branch
    U.S. Department of the Coast Guard
    Research and Development Center
    Avery Point, Connecticut 06340

59. Science Applications, Inc.
    Attn: Dr. Robin Muench   1
    13400B Northrup Way
    Suite 36
    Bellevue, Washington 98005

60. Institute of Polar Studies
     Attn: Library   1
     103 Mendenhall
     125 South Oval Mall
     Columbus, Ohio 43210

61. Institute of Marine Science
     University of Alaska
     Attn: Library   1
     Fairbanks, Alaska 99701

62. Department of Oceanography
     University of British Columbia
     Attn: Library   1
     Vancouver, British Columbia
     CANADA
     V6T 1W5

63. Institute of Marine Science
     University of Alaska
     Attn: Dr. H.J. Niebauer   1
     Fairbanks, Alaska 99701

64. Bedford Institute of Oceanography
     Attn: Dr. P. Jones   1
            Library   1
     P.O. Box 1006
     Dartmouth, Nova Scotia
     CANADA
     B2Y 4A2

65. Carol Pease   1
     Pacific Marine Environmental Lab/NOAA
     7600 Sand Point Way N.E.
     Seattle, Washington 98115

66. Department of Oceanography   1
     Dalhousie University
     Halifax, Nova Scotia
     CANADA
     B3H 4J1

67. Dr. Richard Armstrong   2
     MIZEX Data Manager
     National Snow and Ice Data Center
     Cooperative Institute for Research
      in Environmental Sciences
     Boulder, Colorado 80309

106

68. Institute of Ocean Sciences
    Attn: Dr. Eddy Carmack   1
          Dr. E. L. Lewis   1
          Dr. G. Holloway   1
    P.O. Box 6000
    Sidney, British Columbia
    CANADA
    V8L 4B2

70. Dr. Knut Aagaard   1
    NOAA/PMEL
    NOAA Bldg. #3
    7600 Sand Point Way, N.E.
    Seattle, Washington 98115

71. Department of Ocean Engineering   1
    Attn: Library
    Mass. Institute of Technology
    Cambridge, Massachusetts 02139

72. Dr. Theodore D. Foster   1
    Center for Coastal Marine Studies
    University of California
    Santa Cruz, California 95064

73. Research Administration   1
    Code 012
    Naval Postgraduate School
    Monterey, California 93943-5000

74. Dr. Hugh D. Livingston   1
    Woods Hole Oceanographic Institution
    Woods Hole, Massachusetts 02543

75. Dr. T.O. Manley   1
    Lamont-Doherty Geological Observatory
    Palisades, New York 10964

76. Dr. A. Foldvik   1
    Geophysical Institute
    University of Bergen
    Bergen, NORWAY

77. Dr. Preben Gudmandsen   1
    Electromagnetics Institute
    Technical University of Denmark
    Building 349
    DK-2800 Lyngby, DENMARK

78. Dr. D. Hanzlick   1
    Flow Industries, Inc.
    Kent, Washington 98064

79. Dr. W.D. Hibler   1
    Thayer School of Engineering
    Dartmouth College
    Hanover, New Hamsphire   03755

80. Director General Fleet Systems   1
    Attn: Ivan Cote'
    Canadian Coast Guard
    Tower A, Place de Ville
    Ottawa, Ontario
    Canada K1A 0N7

81. Mr. Tom Cocke   1
    Office of Marine Science
    U.S. Department of State
    Washington, D.C.   20525

82. Commanding Officer   1
    CCGS SIR JOHN FRANKLIN
    Canadian Coast Guard Base
    P.O. Box 1300
    St. John's Newfoundland
    Canada A1C 6H8

83. M. Kim O. McCoy   1
    SeaMetrics
    9320 Chesapeake Dr., #212
    San Diego, CA   92123

84. CDR Erik Thomsen   1
    Danish Liaison Office
    Thule AFB
    Thule, Greenland

85. LT V. G. Addison, Jr.   5
    46 Division Avenue
    Massapequa, N.Y.   11758

86. LT A.M. Weigel   1
    4332 Great Oak Drive
    Charleston, SC   29418

87. Research Administration   1
    Code 012
    Naval Postgraduate School
    Monterey, CA 93943-5000

88. Superintendent   2
    Naval Postgraduate School
    Attn: Library (Code 0142)
    Monterey, California 93943-5002

END

DATE

FILMED

DTIC

4/88